Development of Al-Fe_3Al Composites by Powder Metallurgy Route

Dissertation submitted to the

National Institute of Technology Rourkela

in partial fulfillment of the requirements

of the degree of

Master of Technology (Research)

in

Metallurgical and Materials Engineering

by

Deepankar Panda
(Roll Number-613MM3015)

Under the supervision of

Dr. Syed Nasimul Alam

and

Dr. Pitamber Mahanandia

August, 2016

Department of Metallurgical and Materials Engineering
National Institute of Technology Rourkela

Metallurgical and Materials Engineering
National Institute of Technology Rourkela

August, 2016

Certificate of Examination

Roll Number: 613MM3015
Name: Deepankar Panda

Title of Dissertation: Development of Al-Fe_3Al Composites by Powder Metallurgy Route

We the below signed, after checking the dissertation mentioned above and the official record book (s) of the student, hereby state our approval of the dissertation submitted in partial fulfillment of the requirements of the degree of Master of Technology (Research) in Metallurgical and Materials Engineering at National Institute of Technology Rourkela. We are satisfied with the volume, quality, correctness, and originality of the work.

Pitamber Mahanandia
Co-Supervisor

Syed Nasimul Alam
Principal Supervisor

Samir Kumar Acharya
Member (MSC)

Santosh Kumar Sahoo
Member (MSC)

Debasis Chaira
Member (MSC)

External Examiner

Subash Chandra Mishra
Chairman (MSC)

Metallurgical and Materials Engineering
National Institute of Technology Rourkela

August, 2016

Supervisors' Certificate

This is to certify that the work presented in this dissertation entitled "*Development of Al-Fe_3Al Composites by Powder Metallurgy Route*" by "*Deepankar Panda*", Roll Number 613MM3015, is a record of original research carried out by him under our supervision and guidance in partial fulfilment of the requirements of the degree of *Master of Technology (Research)* in *Metallurgical and Materials Engineering.* Neither this dissertation nor any part of it has been submitted for any degree or diploma to any institute or university in India or abroad.

---------------------------------	-----------------------------
Pitamber Mahanandia	*Syed Nasimul Alam*
Co-Supervisor	Principal Supervisor

Declaration of Originality

I, *Deepankar Panda,* Roll Number *613MM3015 hereby* declare that this dissertation entitled "*Development of Al-Fe_3Al Composites by Powder Metallurgy Route*" represents my original work carried out as a postgraduate student of NIT Rourkela and, to the best of my knowledge, it contains no material previously published or written by another person, nor any material presented for the award of any other degree or diploma of NIT Rourkela or any other institution. Any contribution made to this research by others, with whom I have worked at NIT Rourkela or elsewhere, is explicitly acknowledged in the dissertation. Works of other authors cited in this dissertation have been duly acknowledged under the section "Bibliography". I have also submitted my original research records to the scrutiny committee for evaluation of my dissertation.

I am fully aware that in case of any non-compliance detected in future, the Senate of NIT Rourkela may withdraw the degree awarded to me on the basis of the present dissertation.

August, 2016

NIT Rourkela *Deepankar Panda*

Acknowledgement

It is a privilege for me to express my profound gratitude and indebtedness to my supervisors Dr. S. N. Alam, Metallurgical & Materials Engineering Department and Dr. P. Mahanandia, Department of Physics and Astronomy, National Institute of Technology Rourkela. Without their effort and guidance this work could not have been possible. They have guided me at all stages during this research work. I will cherish all the moments of enlightenment they have shared with me.

I would like to convey my sincere gratitude to Prof. S.C. Mishra, Head of the Department, Metallurgical and Materials Engineering Department, National Institute of Technology Rourkela, for his constant guidance and encouragement. I would also like to express my sincere thanks to Dr. A. Basu and Dr. S. K. Karak for constantly encouraging me and helping me understand my research problem. I am very much thankful to Dr. N. Yedla and Dr. K. Dutta for giving valuable suggestions during the period of my work. I would also take the pleasure of thanking all my master scrutiny committee members, Dr. S. K. Acharya, Dr. D. Chaira and Dr. S. K. Sahoo for assessing my research work and providing me valuable suggestions throughout the work.

I am also thankful to Mr. Rajesh Pattanaik, Mr. U. K. Sahu, Mr. S. Chakraborty, Mr. S. Pradhan, Mr. Kishore Tanty, Mr. S. Hembram, Mr. Anup Acharya and Mr. Arindam Pal of NIT Rourkela for their technical guidance in conducting various experimental studies during the research work.

I am also thankful to my friends Lailesh Kumar, Deepanshu Verma, Harshpreet Singh, Pallabi Bhuyan, Prekshya Nath, Kishore Kumar Mahato, Anil K. Bankoti, Himanshu Sekhar Maharana, Snehashish Tripathy, Rakesh Sahoo and Dhananjaya Sahu for their help and support during my research work.

I am grateful to my brother in-law Mr. Sanjay Dhal for his love, affection and understanding. He has provided constant support throughout the period of my study. Special thanks to my parents and my sisters for motivating me and assisting me. Without their help and encouragement it would not have been possible for me to undertake this work. I would like to thank all my friends for making my stay at NIT Rourkela lively and without their help this work would not have been possible.

August, 2016 — *Deepankar Panda*

NIT Rourkela — Roll Number: 613MM3015

Abstract

Aluminium based MMCs are one of the most prominent materials due to their low density, high specific strength and stiffness and increased fatigue resistance which make them suitable for various wear and structural applications in various aerospace and automotive industries. Aluminium (Al) is widely used due to its excellent properties such as low density high thermal and electrical conductivity. However, Al has poor wear resistance behaviour, low hardness and poor fatigue properties. This is why Al is very often reinforced with hard materials like carbides, borides, nitrides, oxides and intermetallics. Rising interests in intermetallic compounds is connected with their high strength, corrosion resistance and wear resistance. Among the several intermetallic compounds available iron aluminide (Fe_3Al) has been frequently considered for high-temperature structural applications because of their unique physical and mechanical properties. Fe_3Al intermetallic compound has a high melting point, high hardness, low density and good oxidation and corrosion resistance. In the present work, an attempt has been made to study the effect of addition of Fe_3Al as reinforcement in Al metal matrix composites. Here, in the present research work Al-10, 20, 30 vol. % Fe_3Al composites have been developed by powder metallurgy route and their microstructure, hardness and wear properties have been investigated. In the present research work both as-received Fe_3Al and Fe_3Al developed by 40 h of mechanical alloying (MA) of $Fe_{75}Al_{25}$ powder followed by heat treatment at 1100^{o}C for a period of 2 h in Ar atmosphere has been used as reinforcement. Nanocrystalline Al developed by milling Al powder for a period of 20 h has been used as the matrix for all the Al-Fe_3Al composites developed in this study. The milled powders were analyzed using x-ray diffraction (XRD), scanning electron microscope (SEM), energy dispersive x-ray spectroscopy (EDX), high resolution transmission electron microscope (HRTEM), differential scanning calorimetry (DSC) and thermogravimetric analysis (TGA). The 20 h milled nanocrystalline Al was mixed with both the as-received Fe_3Al powder and the Fe_3Al powder synthesized by MA in different vol. % and compacted under a uniaxial load of 222 MPa and sintered at 500^{o}C for a period of 2 h in Ar atmosphere. The microstructure of the various Al-Fe_3Al sintered composites was analyzed using optical microscope, SEM and EDX. The relative density of the various sintered composites was determined by the Archimedes' principle. Dry sliding wear test of the various sintered composites was done on a ball-on plate tribometer to determine the wear behaviour of the composites. The hardness of the composites was determined using a Vickers microhardness tester. It was found that both the hardness and the wear resisiatnce of the various Al-Fe_3Al sintered composites increased with the increase in Fe_3Al content.

Keywords*: *Mechanical Alloying*; *Al-based MMCs*; *Iron Alumindes*; *Wear*; *Hardness.

Contents

List of Figures

List of Tables

Chapter 1

Introduction

1.1 Motivation and Background

The need for new materials which can be used under adverse environmental conditions has led to the discovery of new materials. Modern technologies require materials having a combination of many properties such as high strength, light weight, high toughness, corrosion resistance, high abrasion, impact resistance etc. To inculcate the above properties into a single material, composite materials came into existence. A composite comprises of two or more different materials that are combined together to create a superior and unique material. In simple words, a composite can be described as a multiphase structural material that consists of two or more chemically different constituents which are blended at macroscopic level. The history of composites dates back to ancient times. In ancient times, generally mud bricks were used as a building material. However, these bricks were prone to breakage, when they were bent. To overcome the problems the mud bricks were reinforced with a strong phase like straw. Straw was mixed with mud to form a building material known as adobe. Straw provides the structure and strength, while mud acts as a binder, holding the straw together in place. The above combination made the bricks better resistant to squeezing and tearing, thus making them suitable for building purposes.

The need for composite materials is growing day by day. Today industries like aerospace, automobile, underwater transportation, sports equipment etc. require materials having the unusual combination of both strength and stiffness. To meet the demands of these industries, composite materials have gained importance. Superior property combinations could be achieved with the development of composite materials. Usually composite materials are composed of two phases, matrix and reinforcement. Matrix is the dispersed phase which surrounds the reinforcing phase. The matrix phase is generally light, ductile and continuous whereas the reinforcing phase is strong, hard and discontinuous. The reinforcement can take up any form like fibers, particles or flakes. Composites obey the rule of mixtures which states that the properties of a composite system are highly governed by the relative proportion and properties of the constituent phases. Materials could therefore be designed according to the need of properties by varying the volume fraction of the constituent phases. Some natural composites are wood, bone etc. Wood is a fibrous composite composed of cellulose fibres reinforced in lignin matrix. Cellulose fibre has high tensile strength and is reinforced in a stiffer material called lignin that also provides better links between the matrix and fibers. Similarly bone is also a natural composite composed of short and soft collagen fibres surrounded by mineral matrix called apatite. Concrete is also a commonly used composite material. It is an aggregate of small stones, cement and sand. To increase the tensile strength of the concrete, a combination of the concrete and metal rods or wires has been developed. The above composite is widely known as reinforced concrete [1–3].

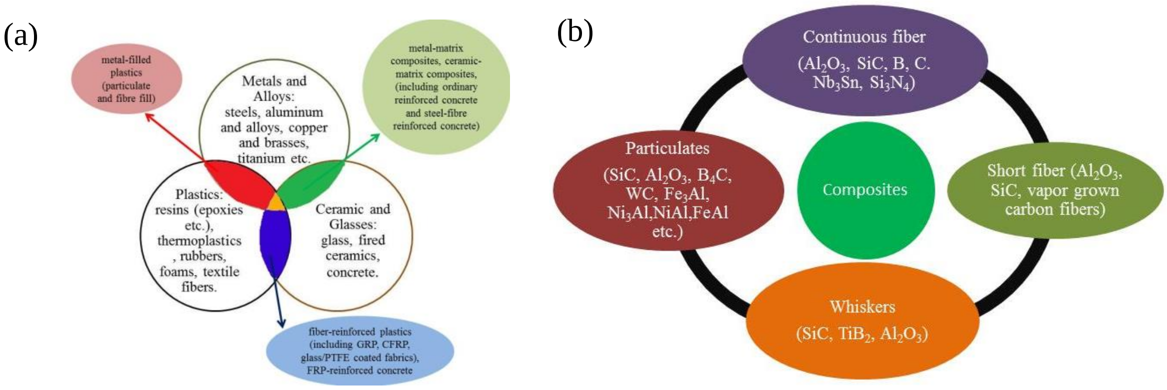

Figure 1.1: (a) The relationship between the various classes of engineering materials showing the evolution of composites (b) Various types of reinforcements used in composites

1.1.1 Properties of Composites

Composite materials include some of the most advanced engineering materials today. Composite is a class of materials which receive a large attention because of their outstanding properties and their potential applications in a wide range of industries. By combining two or more distinct materials one can develop a new material with the desired combination of properties. This could lead to materials having a combination of properties like light weight, high strength, corrosion resistance etc. [4,5]. The following properties of composites make them a promising material to be used in various applications:

High Strength to Weight Ratio

A composite material is the only material which can be designed to achieve both strength and stiffness. This enhanced combination of properties makes them popular in the automotive and aerospace industries. Today composites are one of the most popular materials which show better strength to weight ratio. Composites are lighter in weight as compared to most conventional metals, alloys and ceramics. Being lighter in weight, composites can be used to make light weight vehicles which can provide better fuel efficiency. A net weight reduction of around 20-50 % is achievable by using composites.

Strength

Strength is the most vital property of the material when it comes to application in industries like automobiles and aerospace. Composites are capable of replacing metals as well as ceramics in a large number of areas by optimizing the mechanical properties. A composite material combines the superior properties of both the matrix and the reinforcement and thus possesses enhanced properties in contrast to monolithic materials. Composite materials not only reduce the weight and manufacturing cost of the material, but also improve creep strength, fatigue strength, toughness, oxidation and corrosion resistance and high temperature properties.

Corrosion Resistance

Composite materials have good weathering properties and resist the attack of a wide range of chemicals. Composites are the best choice for applications where corrosive environments are involved. To diminish metal loss rate during corrosion, composite materials play a vital role. They resist metal loss under adverse environmental conditions and from harsh chemicals that erode away other materials. This is why composites are used for the manufacture of chemical storage tanks, pipes, chimneys and ducts, boat hulls and vehicle bodies.

Lower Assembly Cost

Composites are not only preferable due to their excellent properties, but also because of their lower the manufacturing cost.

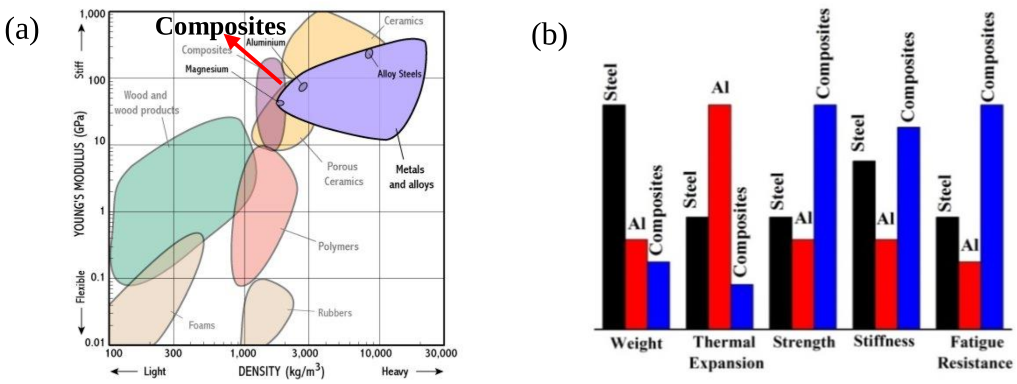

Figure 1.2: (a) Young’s modulus of various types of materials (Ashby Plot) (b) Comparison of various properties of steel, Al and composites

Figure 1.2 (a) and (b) show young's modulus of various types of materials and comparison of various properties of steel, Al and composites respectively. The Ashby plot in Fig.1.2 (a) is very clearly shows the range of modulus values of different types of materials. On the basis of the types of matrices composites can be classified into three main categories:

1. Metal matrix composites (MMCs)
2. Ceramic matrix composites (CMCs)
3. Polymer matrix composites (PMCs)

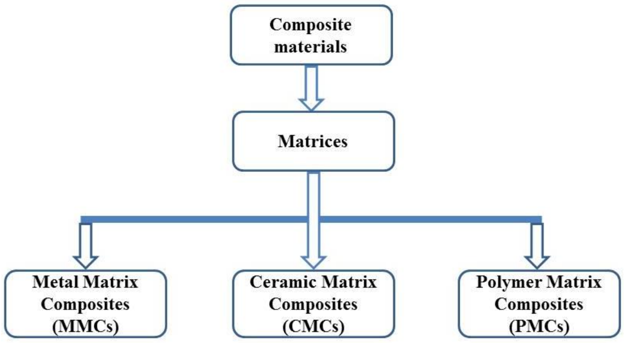

Figure 1.3: Classification of composites based on matrices

1.2 Metal Matrix Composites (MMCs)

In recent years MMCs have gained noticeable importance in the field of engineering materials and has been used in several applications in aerospace and automotive industries. MMCs usually consist of a low-density metal reinforced with particulates or fibers of ceramic material. Compared with unreinforced metals, MMCs offer higher specific strength and stiffness, higher operating temperature, and greater wear resistance. MMCs show superior mechanical properties, such as high hardness, better tensile strength, high elastic modulus etc. along with better thermal stability at higher operating temperatures as compared to unreinforced metals and alloys. In general, MMCs can be classified into discontinuously reinforced MMCs and continuous fiber or sheet reinforced MMCs. Among all the MMCs, particulate reinforced composites are very popular and extensively used due to their simplicity in manufacturing. MMCs are fabricated by several techniques such as powder metallurgy, liquid metallurgy and squeeze-casting techniques. Among these powder metallurgy is the most economically viable and widely acceptable fabrication technique. This technique provides better compatibility between the matrix and reinforcement phase and also provides homogeneous distribution of the reinforced phase. In the MMCs, the volume fraction of the reinforced particles or whiskers generally lies within the range of 10-50 %. MMCs are the most preferred materials in the field of tribological and structural applications. Due to the synergistic effect of the hard reinforced particulates and the ductile metal matrix, the particulate reinforced metal matrix composites exhibit excellent tribological property. Wear mechanism is based not only on the mechanical but also on the thermal and chemical interaction between the two contacting surfaces. High wear resistance can only be achieved by hard ceramic and intermetallic particulates because of their high wear resistance and better compatibility with matrix materials. The interfacial characteristics in MMCs show significant role in determination of the composite properties. MMCs have the ability to withstand high tensile and compressive stresses via the transfer and distribution of the applied load from the ductile matrix to the reinforcement phase. These outstanding features make MMCs one of the most prominent materials for structural and high temperature applications [6–8]. In the present research work aluminium based metal matrix composite has been developed by using iron aluminide intermetallic (Fe_3Al) compound as the reinforcement.

1.3 Aluminium based MMCs

Al-based MMCs are one of the most prominent composite materials due to their low density and light weight which make them suitable for various wear and structural applications in aerospace and automotive industries. Al-based MMCs have already been considered as an alternative material for the use in the fabrication of brake rotors, pistons, cylinder liner and cylinder heads. Al is widely used due to its excellent properties such as low density (2.72 gm/cc), high thermal conductivity (237 W/m.K) and high electrical conductivity (3.8×107 S/m). However, Al has poor wear resistance behaviour and its hardness is 167 MPa. Its modulus is 70 GPa and its ultimate tensile strength is 110 MPa. MMCs with hard particles are gaining importance due to enhancement in various properties. This is why Al is reinforced with hard materials like carbides, borides, nitrides, oxides and intermetallics. Al-based MMCs are widely used for sliding wear applications. Apart from being good wear resistant materials, Al-based MMCs also have high specific strength, high specific modulus and superior fatigue and creep resistance which make them suitable for various wear and structural applications. Apart from this Al also provides a compatible environment to foreign particles for better incorporation and good bonding with the reinforcement phase [9, 10].

1.4 Powder Metallurgy

Powder Metallurgy (PM) is a continually and rapidly evolving technology embracing most metals and alloys. By producing parts having a homogeneous structure the PM process enables manufacturers to develop products that consistent and predictable in their behaviour across a wide range of applications. It is a highly energy-efficient and cost-effective process for the production of near-net shape products having a wide range of alloy compositions. The PM process has a high degree of flexibility and allows tailoring of physical characteristics of a product to suit specific property and performance requirements. By producing parts with a homogeneous structure the PM process enables manufacturers to make products that are more consistent and predictable in their behaviour across a wide range of applications. The PM process is typically useful for high temperature resistive materials which have high melting points, like Titanium (Ti), Tungsten (W) etc. Now days this unique technique gaining much more attention for the manufacturing of complex geometrical shapes with maximum material utilization and reduced processing steps. The different stages involved in powder metallurgy are: (1) Blending of powder mixtures (2) Compaction of powders in a die to produce green pellets (3) Sintering of green pellets at a temperature to the point of liquefaction in a controlled furnace atmosphere to bond the powder particles metallurgically [11].

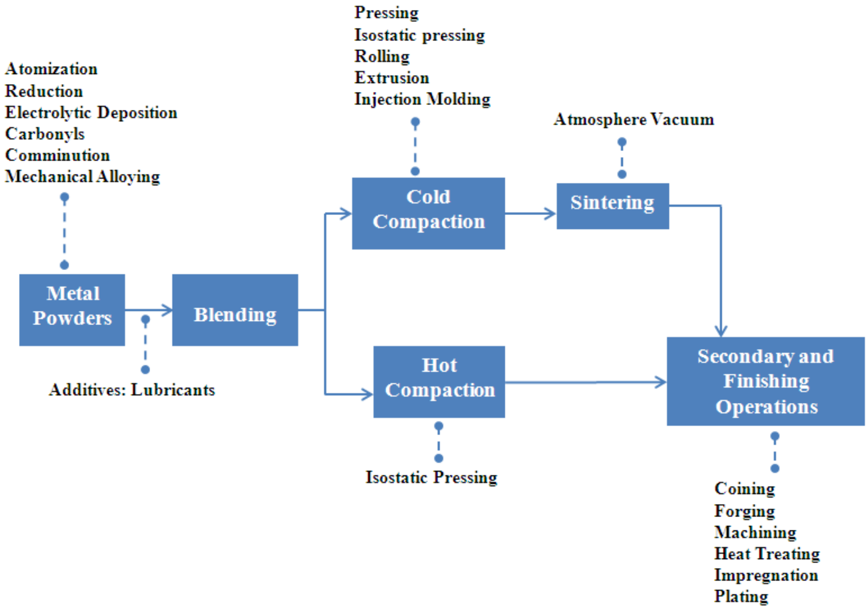

Figure 1.4: A flowchart of the basic processes involved in powder metallurgy

1.5 Mechanical Alloying (MA)

Mechanical alloying (MA) is used as one of the preferred method for powder processing. MA is a solid-state powder processing technique which involves repeated welding, fracturing, and rewelding of powder particles in a high-energy planetary ball mill. It was originally developed to produce oxide-dispersion strengthened (ODS) nickel- and iron-based superalloys for applications in aerospace industries. John Benjamin and his colleagues at the Paul D. Merica Research Laboratory of the International Nickel Company (INCO) developed the process in around 1966. This technique was the result of an extended search to develop nickel-based superalloys for gas turbine applications. The mechanical alloying process was highly successful in producing ODS alloys with better high temperature capabilities in comparison with other processing techniques.

MA produces homogeneous materials with dispersed and uniform internal structure. It is very difficult to fabricate high melting intermetallics by conventional processing techniques. However, they could be easily fabricated by mechanical alloying with homogeneous distribution of blended powder particles. The maximum probability of attaining solid solubility in liquid immiscible systems has been observed by MA process. The diffusion of mechanical energy to the powder particles during MA results in introduction of strain in the powder. This energy generates dislocations and other defects which act as fast diffusion paths. MA is capable of synthesizing a variety of equilibrium and non-equilibrium alloy phases. The non-equilibrium phases synthesized include supersaturated solid solutions, metastable crystalline and quasicrystalline phases, nanostructures, and amorphous alloys. Reactive milling has shown new ways for the solid state metallothermic reduction, synthesis of nanocrystalline intermetallic and various metal matrix composites. In recent years MA has also been extensively used in synthesis of nanocrystalline materials, nanocomposites and intermetallic compounds. In addition to this many quasicrystalline phases have also been produced in many metallic systems by using MA technique. Generally MA is done in a dry condition under an inert atmosphere to prevent the oxidation of the powders. To prevent excessive cold welding of particles in the case of ductile materials such as Al and Sn, process control agents (PCAs) are used**.** The PCAs are mainly organic materials such as stearic acid, methanol, and toluene and are used to attain proper balance between cold welding and fracture of powder particles. Figure 1.5 shows the collision of ball-powder-ball collision during high energy ball milling [12-16].

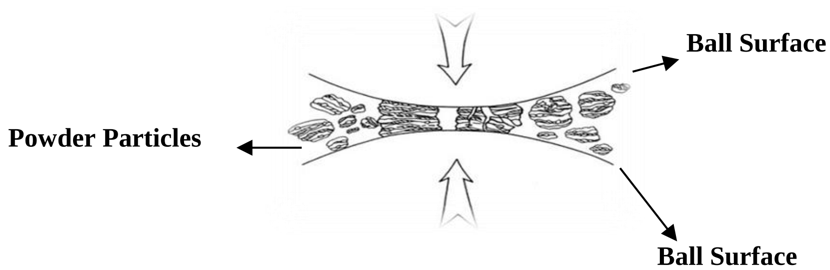

Figure 1.5: Ball-powder-ball collision during high energy ball milling

1.6 Intermetallic Compounds

An intermetallic compound is widely known as a solid state compound having a long range ordered structure exhibiting high metallic bonding. They are materials composed of two or more metallic elements, producing a new phase having same composition, crystal structure and properties. The crystal structures of intermetallic compounds are noticeably different from that of its constituents. They exist as homogeneous, composite substances and differ in structure from that of the constituent metals. Intermetallics are gaining importance due to their novel attributes such as excellent high temperature strength, thermal stability, high corrosion and oxidation resistance. They are very hard and brittle similar to ceramic materials. Intermetallic compounds are analogous to ceramics when it comes to high temperature stability. The main reasons to incorporate intermetallic compounds in the matrices are their high hardness and high wear resistance. The high hardness of intermetallic compounds is attributed to the fact that they possess a complex crystal structure and as a result, have very less number of slip planes which are active during the process of plastic deformation. Intermetallic compounds are not only popular for their hardness and wear resistance but also for their good compatibility with the metal matrix of composites which make them more suitable for the tribological applications. Due to their high melting temperature it is very difficult to fabricate intermetallic compounds through casting. Mechanical alloying has been found to be an extremely promising technique for the synthesis of intermetallic compounds. The intermetallics having the compositions Fe_3Al, FeAl, $FeAl_2$, Fe_2Al_3, Fe_2Al_5 and $FeAl_3$ can be found in the binary Fe-Al phase diagram in Figure 2.5. Out of these Fe_3Al and FeAl are of interest for structural applications as the rest of the phases are known to be very brittle and metastable in nature [17].

1.6.1 Aluminides

Aluminides are one of the most widely used intermetallics. Due to their excellent high temperature properties aluminides are widely used in aerospace and automotive industries. Among all aluminides, nickel, titanium and iron aluminides have so far gained major consideration. A keen interest in the synthesis of aluminides by mechanical alloying (MA) has risen as MA has been found to be a very favourable processing technique for their synthesis. The formation of nickel aluminides, such as NiAl and Ni_3Al via MA has been confirmed at various compositions in binary Ni_xAl_{100-x} ($32 < x < 90$) elemental blends. Ni_2Al_3 and Ni_5Al_3 phases are found to be metastable in nature under similar conditions. The formation of titanium aluminides can be achieved by adopting a two-step process which comprises of MA and subsequent annealing. The various titanium aluminides are TiAl, $TiAl_3$ and Ti_3Al, which can be formed by MA under a proper stoichiometric composition. Iron aluminides are mainly two types, one is aluminium rich, i.e., Al_3Fe and another is iron rich, i.e., Fe_3Al and FeAl. Other aluminides can be found in systems like, Al-Nb, Al-Mo, Al-Zr, Al-Ni-Fe, etc [17, 33-36].

Iron Aluminides

There are a number of intermetallics such as, Au_2Pb, AlSb, $MoSi_2$, Mg_2Pb, $CuAl_2$, $TiAl_3$, Fe_3Al, FeAl, Ni_3Al, NiAl, Fe_3C etc. Among these iron aluminides (Fe_3Al, FeAl) have been frequently considered for high temperature structural applications because of their unique physical and mechanical properties. They have high melting points, low density, excellent mechanical properties and high corrosion resistance. Apart from this they are also low cost materials. In the present work, an attempt has been made to study the effect of addition of Fe_3Al as reinforcement in Al metal matrix composites.

Fe_3Al intermetallic compound has a high melting point (1540 ^oC), high hardness (338 HV), low density (6.72 g/cc) and good oxidation and corrosion resistance. Furthermore the yield strength of Fe_3Al increases with the increase in temperature upto 600 ^oC. Fe_3Al could also act as a low cost material alternative to stainless steel. They can easily sustain corrosive atmosphere by forming an adherent surface film of Al_2O_3. It also has a higher ductility as compared to stainless steel. High yield strength, high ultimate tensile strength, excellent resistance to highly oxidizing molten salts as well as good sulfidation resistance at high temperatures makes Fe_3Al an ideal reinforcement material. Composites with Fe_3Al as reinforcement exhibit high strength as compared to many ferritic and austenitic stainless steels which makes them an attractive candidate material for high temperature applications. Iron aluminide (Fe_3Al) reinforced composites show improved wear resistance under dry sliding conditions. However, very few works have been reported in literature on Al-Fe_3Al MMCs developed by powder metallurgy route. In the present research work, as-received Fe_3Al powder as well as Fe_3Al synthesized by mechanical alloying has been used as reinforcement for the development of Al-Fe_3Al composites.

1.7 Scope and Objectives of the Present Research

The aim of the present research work is to develop Al-based MMCs using iron aluminide (Fe_3Al) as reinforcement by powder metallurgy route having superior mechanical and tribological properties.

The major objectives of the present research work are:

i. To synthesize nanostructured Al powder by mechanical milling of elemental Al powder. The nanostructured Al will be used as the matrix for the development of the various Al-Fe_3Al composites.
ii. Synthesis and characterization of Fe_3Al intermetallic compound developed by mechanical alloying (MA) of $Fe_{75}Al_{25}$ powder in a high energy planetary ball mill followed by isothermal annealing of the milled powder.
iii. To develop Al-Fe_3Al MMCs using both as-received Fe_3Al powder and Fe_3Al synthesized by MA of $Fe_{75}Al_{25}$ powder followed by isothermal annealing of the milled powder as reinforcements.
iv. To study the effect of addition of Fe_3Al as reinforcement on the mechanical and tribological properties of the Al-Fe_3Al composites.

1.8 Thesis Outline

The thesis includes five chapters. **Chapter 1**, **"Introduction"**, provides a brief introduction of composites, Al-based MMCs, powder metallurgy, mechanical alloying (MA), intermetallic compounds and iron aluminides. **Chapter 2**, **"Literature Survey"**, throws light on the work that has been carried out by other researchers in this field and presents a comprehensive literature review available in this area. **Chapter 3**, **"Experimental Procedure"**, includes the various experimental procedures that have been used in the present research work and the prescribed experimental norms. **Chapter 4**, **"Results and Discussion"**, presents the detailed analysis of the results that have been obtained in the present research work. This chapter elucidates and analyses the outcomes and findings of the present work. **Chapter 5**, **"Conclusions"**, lists the various conclusions that have been drawn from the results of this research work.

● ● ● ●

Chapter 2

Literature Survey

2.1 Composites

A composite is a material produced, when two or more constituent materials with significantly different physical or chemical properties are combined as a result of which the properties of the composite are improved as compared to the individual constituents themselves. The individual constituents remain distinct within the composite. The main two phases in a composite are the matrix and the reinforcement. A wide variety of matrix and reinforcement materials are available. To achieve the desired properties an optimum combination of the matrix and the reinforcement are done. The matrix phase is usually soft and ductile in nature whereas the reinforcement phase is harder, stronger and stiffer as compared to the matrix phase. A good bonding between the matrix and the reinforcement phase provides better strength and stiffness to the composite materials. Usually matrix phases are continuous that surround and bind the discontinuous reinforcement phases. The matrix plays an important role during the distribution of stresses to the reinforcement phase. The reinforcements provide superior physical and mechanical properties to enhance the properties of the matrix phase. However, the type of reinforcement and its orientation in the matrix alters the properties of the developed composite and hence must be carefully chosen as per the requirement of the application. Composites allow us to have tailorable mechanical properties. High strength and stiffness combined with light weight make composites very popular. Composite materials are used in industries like aerospace, automotive, sporting goods, home appliances etc. Figure 2.1 (a) shows the different types of reinforcements that can be incorporated inside the matrix phase and Figure 2.1 (b) shows the classification of composite materials on the basis of types of reinforcements. The reinforcement can be in the form of particulates, short fibers or continuous fibers, which are well bonded with the matrix within the composites [18, 19].

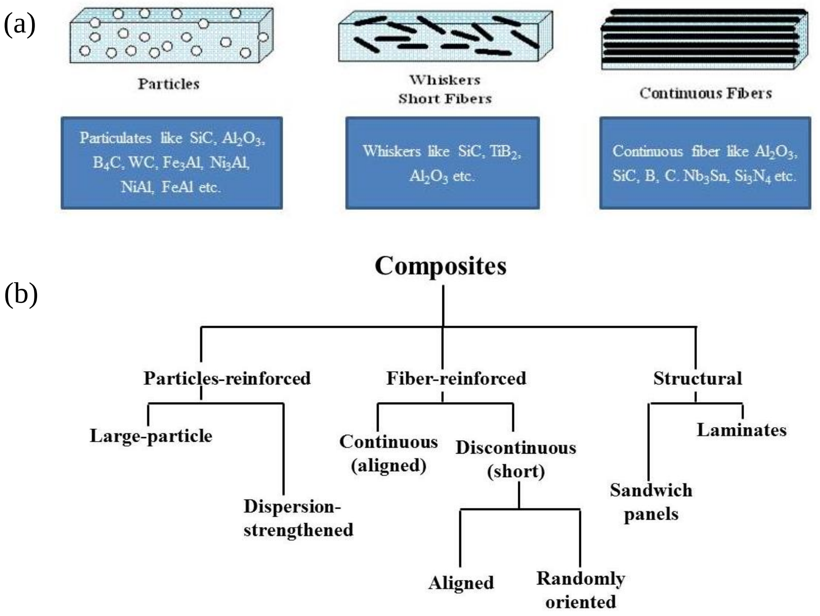

Figure 2.1: (a) Various types of reinforcements (b) Classification of composite materials on the basis of types of reinforcements

2.2 Metal Matrix Composites (MMCs)

Conventional monolithic materials have limitations in achieving a good combination of strength, stiffness, toughness and density. To overcome these limitations development of metal matrix composites (MMCs) have gained more importance in aerospace and automotive industry. MMCs usually consist of metal having low-density, such as aluminum or magnesium, reinforced with particulates or fibers of a ceramic material. The selection of the matrix metal or alloy is determined mainly by the application of the composite. Compared with unreinforced metals or alloys, MMCs are capable of providing high specific strength, high stiffness, higher operating temperature, greater wear resistance as well as the opportunity to tailor these properties for a particular application. These desirable properties make them favorable material over conventional monolithic materials for several applications. MMCs are composite materials with at least two constituent parts one being a metal. To accomplish optimum mechanical and physical properties, it is necessary to achieve uniform distribution of the reinforcement within the metal matrix. They are produced by dispersing a reinforcement material uniformly in to the metal matrix. The reinforcement can be either continuous or discontinuous. The major difference between the fiber and particulate reinforced composites is the directionality of the properties. Particulate reinforced composites show isotropic behavior while fiber reinforced composite are usually anisotropic. Due to their isotropic nature particulate reinforced composites deliver higher ductility which makes them an attractive alternative material as compared to fiber reinforced composite. The objective behind the development of light metal matrix composite materials are to achieve higher yield strength and tensile strength at room temperature and above while maintaining the minimum ductility, increase the creep resistance at higher temperatures compared to that of conventional metals and alloys, increase fatigue strength, improve thermal shock resistance, improve corrosion resistance etc. The choice of the reinforcement to be used in a MMC mainly depends on the production and processing and the matrix system of the composite material. Reinforcements for MMCs should have low density, good chemical and mechanical compatibility with the metal or alloy, high modulus of elasticity, high thermal stability, high compression and tensile strength, low cost etc. For the production of MMCs many processing techniques like powder metallurgy, casting or liquid infiltration, compo casting, squeeze casting, pressure infiltration, spray decomposition and stir casting are used [20-22].

2.3 Processing Techniques for MMCs

Metal matrix composites (MMCs) are engineered combination of two or more materials, one of which is a metal where tailored properties can be achieved by a systematic combination of the different constituents. The main purpose of development of MMCs is to combine the desirable properties of metal and a ceramic or an inorganic reinforcement to produce a unique material which has high strength and stiffness as well as low density. Here, the metal acts as a matrix and the ceramic or the inorganic compound acts as reinforcement. Several factors have to be considered for the fabrication of MMCs. These factors include (i) choices of matrices and reinforcements (ii) compatibility between the matrix and the reinforcement (iii) shape, size, orientation and distribution of reinforcements within the matrices (iv) mechanical properties of reinforcements and matrices (v) dimensional tolerances of the product, (vi) cost and applications of the composite developed etc. Based on the state of existence of the matrix metal, there are mainly two types of fabrication routes for the development of MMCs. Figure 2.2 given below lists the various solid state and liquid state processing techniques [23-26].

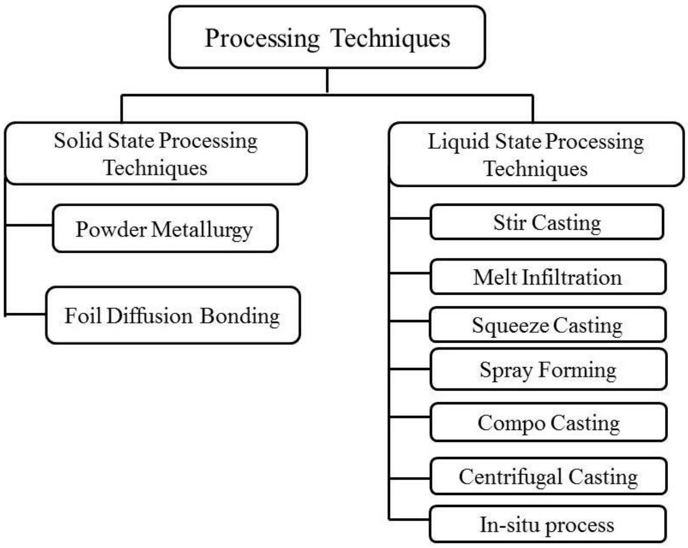

Figure 2.2: Types of fabrication routes for MMCs

2.3.1 Liquid State Processing Techniques

Liquid state processing technique is a process used for forming high performance, multiple-phase components for powders. It involves sintering under specified conditions where solid grains coexist with a wetting liquid. Development of MMCs by liquid state processing techniques is relatively easier as compared to solid state processing techniques. The liquid state processing technique comprises incorporation of reinforcements within the molten metal matrices. There are several advantages in using liquid state processing techniques like, near net shaped final product, higher production rate, dense matrices and better wetting of reinforcements with the matrices. However, liquid state processing techniques also have few drawbacks. In liquid processing techniques, controlling the uniform distribution of reinforcements within the matrices and achieving a uniform microstructure is very difficult. At high temperature, used during liquid state processing, there is also a possibility of adverse reaction between the matrix and the reinforcement at the interface. Due to this reaction some brittle featured compounds are formed which degrade the mechanical properties of composites. Another major problem of the liquid state processing techniques is the segregation of reinforcements due to the difference in the densities between the matrix and reinforcement. Inspite of these disadvantages, liquid state processing techniques are still very popular and are widely used for the production of MMCs. Many variants of the liquid state processing techniques are available for developing a wide range of engineering materials. Few liquid state processing techniques are listed below.

Stir Casting

Stir casting is the simplest and most economical technique for producing MMCs. Stir casting involves mixing of a solid reinforcement in the molten metal followed by solidification in an appropriate mold. During the addition of the reinforcement in the molten metal matrix, the mixture is agitated continuously. After the addition of the reinforcement the viscosity of the molten metal matrix increases. Stir casting involves prolonged melt/reinforcement contact, which can cause interfacial reaction between the melt and the reinforcement. This adverse reaction could form a brittle compound which could degrade the properties of the composites. Stir casting technique is mainly preferred for the development of particulate reinforced composites because long fiber reinforcement is very difficult to cast by using this process. Due to the differences in the densities between the matrix and the reinforcement, continuous stirring is essential to minimize the settling of particulates in the molten metal. Also to avoid oxidation inert gas atmosphere is necessary in stir casting process.

Melt Infiltration

Most casting techniques are not suitable for the development of composites beyond a certain quantity of reinforcement. Melt infiltration technique is the best choice for the production of MMCs containing a high volume or weight fraction of reinforcements. In this technique the metal matrix in liquid form occupies the open spaces within a porous solid. The porous solid is a preform of the reinforcing material which is later infiltrated by the liquid metal matrix. The matrix metal may be in gaseous form rather than liquid form in some processes and MMCs can be produced by chemical vapor infiltration method. The melt infiltration process is faster as compared to other techniques. As compared to the stir casting process the viscosity of the molten metal matrix is not increased after the addition of reinforcement in this process. By using proper preform fabrication method, uniform distribution of reinforcement in all the regions is ensured in this process. Fraction of internal defects in the MMCs can be avoided by using the pressure infiltration technique. However, the major problem of this technique is the tendency for the adverse reaction between the matrix and the reinforcement phase at the interface. So for the reactive systems solid state processing techniques are preferred.

Squeeze Casting

Squeeze casting is a combination of casting and forging process. The molten metal is poured into the bottom half of the pre-heated die. As the metal starts solidifying the upper half closes the die and applies pressure during the solidification process. The pressure applied is significantly less as compared to that in forging and components having excellent feature can be produced by this process. Squeeze casting is the most appropriate process for the production of fibrous reinforced MMCs as it overcomes all the difficulties faced during the production of fibrous reinforced MMCs by liquid state processing. In this method, a reheated composite material or stirred molten mixture is used for the production of MMCs. In this technique pressure is applied over a solidifying composite material along a single direction using a hydraulically activated ram. This results in low porosity levels and fine microstructure. The main difference between the conventional die casting and squeeze casting is the continuous movement of the ram during solidification that deforms the growing dendrite. However, the movement of the ram is slow and a high pressure is applied.

Spray Forming

Spray forming also known as spray casting or spray deposition, is the inert gas atomization of a liquid metal stream into variously sized droplets. These droplets are then propelled away from the region of atomization by the fast flowing atomizing gas. Thereafter the droplets are interrupted by the substrate which collects and solidifies the droplets into a coherent, dense preform. Spray forming technique is a comparatively new technique for the production of particulate reinforced MMCs. This technique employs a spray gun to atomize the molten matrix metal into which reinforcing particulates are inoculated. For effective mixing of the matrix and the reinforcement an optimum particle size is required. This technique involves two stages, spray atomization and spray deposition. In first stage, the molten metal is atomized by the use of highly energetic gas jets onto the substrate surface by disintegrating molten metal into spherical droplets. In the second stage, the molten metal droplets are deposited on the substrate surface. Incorporation of the particulate reinforcements within the molten metal droplets is done to produce the MMCs. Due to extremely short period of interaction, no adverse reaction occurs at the interface between the matrix and the reinforcement. By using this technique a high densification level can be achieved in the composite. Since 1980s a wide variety of MMCS have been developed by this technique. The most widely used matrix materials for this technique are, Al and Al-based alloys, Cu-based alloys, Mg-based alloys and Intermetallics.

In-situ Process

In-situ composites are multiphase materials, where the reinforcing phase is synthesized within the matrix during composite fabrication. Usually MMCs are produced by the incorporation of reinforcements in the metallic matrix, which may be in solid powder or in liquid form. When the reinforcements are fabricated separately before composite fabrication, this process is called as ex-situ process and the MMCs are known as ex-situ MMCs. The main drawbacks of the ex-situ MMCs are the adverse reaction at the interfacial regions of the reinforcements and the matrix. Agglomeration of the particulates and poor wettability of reinforcements with the matrix are the other drawbacks of the ex-situ process. To overcome these drawbacks and to produce MMCs with improved properties in-situ processes have been developed. The in-situ technique removes the problems of non-uniform distribution and poor compatibility of the reinforcement with the matrix. In the in-situ process the reinforcement phases are formed within the metal matrix by the chemical reaction between melt and the solid or gaseous phases during the development of composite. In-situ techniques have several advantages over other manufacturing techniques. For example the reinforcement phases, which are formed within the metallic matrix, are thermodynamically stable. Apart from this, the composites also have clean matrix/reinforcement interfaces resulting in better interfacial bonding. The in-situ process also ensures the uniform distribution of fine structured reinforcements in the matrix, which improves the mechanical properties of the MMCs. In- situ technique, can be classified into two major categories such as, reactive and nonreactive processes. In reactive processes two components react with each other and form the reinforcement phases. Typical examples of the reactive process are TiB_2 and TiC reinforced aluminium alloy composites. Whereas in nonreactive processes matrix and reinforcement phases are formed during solidification. An example of the nonreactive in-situ process is the formation of an aligned two phase structure from a binary alloy melt of eutectic composition on solidification.

2.3.2 Solid State Processing Techniques

Solid state processing techniques are the processes in which the MMCs are formed as a result of the bonding between the metal matrix and the reinforcement due to the mutual diffusion between them in solid state, at an elevated temperature and under pressure. Solid state processes include powder metallurgy, high energy ball milling, friction stir process, diffusion bonding, vapor deposition techniques etc. Solid state fabrication methods are very popular as well as economically viable for the development of MMCs. Near net shaped products can be achieved by adopting these techniques. The final product can be deformed further by rolling, drawing, extrusion, forging etc. at a temperature either below or above the recrystallization temperature.

Diffusion Bonding

Diffusion bonding is a solid state processing technique that is capable of joining both similar and dissimilar metals. It includes the welding of alternating layers of thin metal foil or metal wires. This technique is based on the principle of solid state diffusion. It involves an interaction between the atoms of the two metals over a long period of time under an elevated temperature and high pressure. Diffusion bonding is done by clamping the two metal pieces to be welded with their surfaces adjoining each other. Before welding these metallic surfaces must be smooth and kept away from contamination of any type of chemical constituents. After the clamping of the metallic surfaces, pressure and heating at an elevated temperature are implemented for the production of final product. A hydraulic pressure is given through the ram during heating. Diffusion bonding technique is usually done in an inert atmosphere to prevent oxidation. Diffusion bonding includes no filler metal, so that additional weight is not present. The joint area tends to show both equal strength and high temperature resistance of the base metal. The final product shows little plastic deformation and residual stress, but no contamination from external during diffusion process.

Powder Metallurgy

Powder metallurgy (PM) technique is most simple and economically viable technique and has been developed even before the casting technology. Powder metallurgy technique is an art of producing near net shaped product form the elemental metal powders eliminating or reducing the need for subsequent machining. The powder metallurgy technique is one of the most favourable techniques for materials having high fusion/melting temperature. Powder metallurgy products have controllable porosity and good dimensional accuracy. Nearly 70 % of the products developed by powder metallurgy are for automotive applications. Products developed by powder metallurgy have properties superior to the properties of the two or more metals or non-metals that have been used to develop the product. This unique capability of powder metallurgy process is applied to a number of products. For example, bearings have been developed by powder metallurgy technique by combining graphite with metals like iron and copper or from a mixture of two metals such as, tin and copper, where the harder material provides wear resistance and the softer material deforms in a way which ensures better distribution of load. Powder metallurgy technique has various stages, such as production of metal powders, mixing and blending of powder mixtures in required proportions, compaction of blended powders to produce green pellets and sintering of green pellets in a controlled furnace atmosphere. Metal powders are produced by different processes such as, atomization, reduction, electrolytic deposition, comminution, mechanical alloying etc. Atomization is the process, where a bulk liquid is transformed into fine droplets as produced by impinging jets of air on a stream of liquid which solidifies during the fall through the atomizing tank. It is the process of disintegration of bulk liquids into fine droplets. Commercially atomization is used for the production of large tonnage of metal powders. The major advantages of atomization are (i) ease of making high purity metals and prealloyed powders directly from the melt that can be used solely for powder metallurgy. Almost all metals that can be melted can be atomized (ii) control over particle size and shape (iii) high chemical purity (iv) economically viable and high productivity. Reduction process includes various chemical reactions by which chemical compounds are reduced to elemental powders. In this process a specific reducing agent is used to free the metallic element. This process is generally used to produce powders of Fe, W and Cu. In electrolytic deposition process metal powders are deposited at the cathode from an aqueous solution. By varying the electrolyte composition and other electrical parameters the particle size can be varied over a wide range. The most well-known process for the production of metal powders is mechanical alloying (MA). This process involves charging of two or more metal powders into a high energy ball mill containing a grinding medium of stainless steel, alumina etc. Due to the impact of hard balls repeated cold welding, fracturing, and diffusion of powder particles takes place during the milling operation. After proper mixing of powders, pressing of powders is done by cold compaction or hot compaction in order to produce finished or semi-finished products. The products from compaction are known as green compacts. The green compacts don’t have enough bonding strength between the particles. In order to improve the bonding strength between the particles these green compacts are sintered. Sintering usually involves the thermal treatment of the powder compacts at elevated temperatures, usually at a temperature > $0.5T_m$ K (T_m = melting point of material) where the diffusional mass transport is considerable. As a result a dense solid mass is produced having specific size and shape. The schematic diagram in Figure 2.3 shows the mechanism of the solid state sintering process. During sintering process the diffusion between the particles take place by reducing the distance between the particles and resulting in better bonding. The initial stage of sintering involves the contact between the particles followed by the formation of neck at the point of contact. The intermediate stage involves neck growth and particle centers approaching one another. The final stage of sintering involves elimination of porosity, grain growth and bonding between the particles. The interparticle contact area increases with sintering time. Sintering is an effective process which minimizes the volume of interconnected pores and enhances the properties such as strength and ductility of the sintered product [27-32].

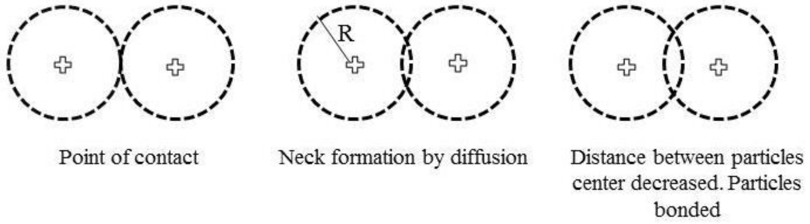

Figure 2.3: Schematic diagram showing the solid state sintering process

2.4 Synthesis of Iron Aluminide (Fe_3Al) by Mechanical Alloying (MA)

A wide variety of methods like hydrogen arc plasma method, self-propagating high temperature synthesis (SHS) method and mechanical alloying (MA) have been used to synthesize Fe-Al intermetallic compounds. Among these methods, MA is the most popular method used to synthesize nanostructured Fe-Al intermetallic compounds. Material transfer by diffusion of components during MA provides the means to synthesize intermetallic compounds. MA is a solid state technique and is especially useful for fabrication of those compounds that are difficult to prepare by conventional processes due to high vapour pressure and/or the large differences in melting point of components. Apart from this during MA synthesis takes place at room temperature. However, MA has few drawbacks like, long periods of milling and chances of contamination from the atmosphere or milling media. Previous works reported by several groups also show that it is possible to obtain bulk intermetallic Fe_3Al phase with a grain refinement upto the nanometer range by properly combining MA with cold consolidation and thermal aging.

Intermetallics are long range ordered alloys having a specific stoichiometric ratio of two or more metals exhibiting metallic bonding. Due to their ordered structure they exhibit superior physical and mechanical properties as compared to an alloy. Iron aluminides are one of the most popular intermetallic compounds. Depending upon the chemical composition iron aluminide has several forms. Figure 2.4 shows the Fe-Al binary phase diagram. At lower concentrations of Al (18-20 at. %) a disordered solid solution of Al in Fe (α) is stable. With the increase in Al concentration two ordered phases of iron aluminide, $D0_3$ and B2, are stable as shown in the binary phase diagram of Fe-Al system. From the binary phase diagram of the Fe-Al system it is evident that there are a number of equilibrium phases such as, the disordered solid solution (α), Fe_3Al with imperfectly ordered B2 crystal structure, ordered Fe_3Al with $D0_3$ crystal structure and the two phase regions, $\alpha+D0_3$ and α+B2. These phases are stable within a wide range of composition. At room temperature the $D0_3$ crystal structure of Fe_3Al intermetallic compound is stable in the composition range of approximately 22-37 at. % Al and can be transformed to the B2 type crystal structure when heated above the $D0_3 \rightarrow B2$ transition temperature (T_c).

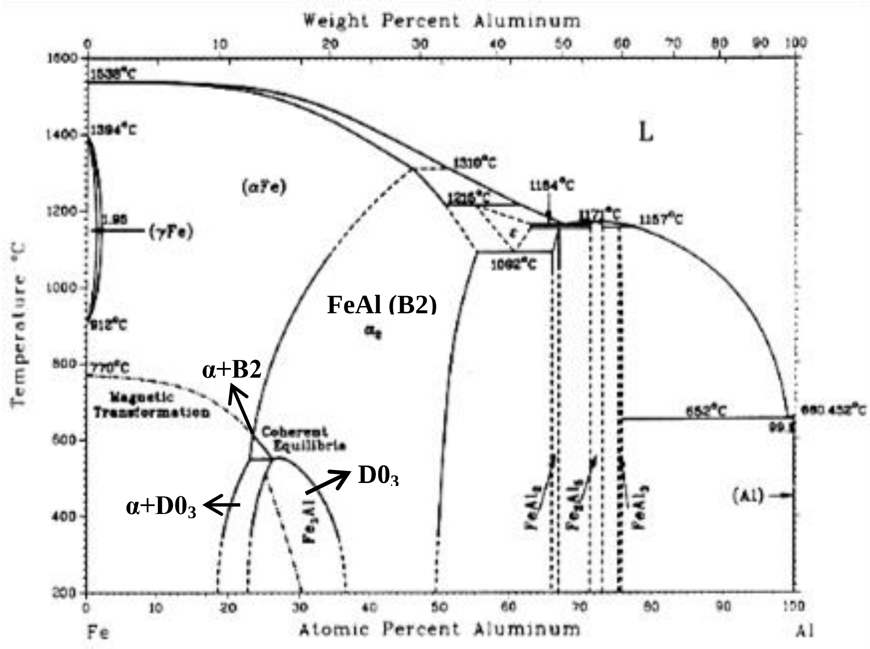

Figure 2.4: Binary phase diagram of the Fe-Al system [33]

The transition temperature for $B2 \rightarrow D0_3$ and vice-versa at the stoichiometric composition of Fe_3Al is approximately 550^oC. This is the critical temperature for ordering. Fe_3Al transforms from an ordered $D0_3$ crystal structure to a defective ordered B2 crystal structure above this temperature. With the rise in Al concentration (approximately above 37 at. % Al) at a room temperature the B2 type crystal structure becomes more stable. FeAl intermetallic compound has B2 crystal structure. The concentration of Al in FeAl varies from approximately 37-50 at. % Al.

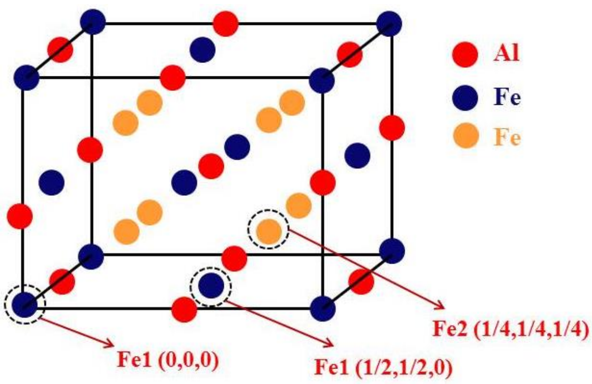

Figure 2.5: $D0_3$ crystal structure of Fe_3Al

Figure 2.5 shows the $D0_3$ crystal structure of Fe_3Al. It is evident from Figure 2.5 that there are two types of Fe atoms. One named as Fe1 has tetrahedral symmetry and can be indexed as (0, 0, 0) and (1/2, 1/2, 0). The other type of Fe atom named as Fe2 has cubic point symmetry and can be indexed as (1/4, 1/4, 1/4). Fe1 atoms have magnetic moment similar to FCC Fe crystal whereas Fe2 atoms have magnetic moment similar to BCC Fe crystal. Al atoms are usually present at body centre position and can be indexed as (1/2, 1/2, 1/2). The $D0_3$ superlattice crystal structure is comprised of eight B2 type superlattices stacked with each other, with alternating Fe and Al as body centred atoms. Al atoms are positioned in such a way that the spacing between them can be maximized with the minimization of energy. This $D0_3$ crystal structure can be viewed as comprised of four nonequivalent interpenetrating FCC sublattices. Generally the production of intermetallic compounds is very difficult as compared to any other alloy due to their high melting points. Mechanical alloying (MA) is the most popular and economically viable process for the development of intermetallic compounds. During milling large plastic deformations occur. This leads to high defect density which initiates the transformation to disordered and/or amorphous state [33, 34].

Murty and Ranganathan [35] have reported that MA is a very promising technique for the synthesis of intermetallics. Among all the intermetallic compounds that have been synthesized by MA, the aluminides have so far received major attention. A large volume of work is available in the literature on the synthesis of Ni, Ti and Fe aluminides by MA. MA of Fe-Al system has been reported earlier in literature by several researchers. Oleszak and Shingu [36] have reported on the MA of Fe-Al powder mixtures in the composition range Fe-10, 20, 30, 40 and 50 at.% Al. They have reported morphological transition of the milled powder from flake-like shape in the initial stages to spherical shape in the final stages after the subsequent isothermal annealing of the milled powder. They have shown by XRD analysis of the Fe-Al milled powder that the (110), (200) and (211) diffraction planes of BCC Fe overlapped with the (200), (220) and (222) diffraction planes of FCC Al. The diffraction planes of Al (111) and (311) having odd miller indices were independent and broadened with increasing milling time. They also reported the disappearance of Al XRD peaks corresponding to diffraction planes having odd miller indices and the increasing trend in the lattice parameter of Fe with the increase in milling time. Enayati and Salehi [37] have also reported about the structural evolution of $Fe_{75}Al_{25}$ and $Fe_{50}Al_{50}$ during MA of elemental mixture of Fe and Al powder in a high energy planetary ball mill under a specific condition. They reported that the MA of $Fe_{75}Al_{25}$ and $Fe_{50}Al_{50}$ initially produced a fine Fe/Al layered microstructure which later transformed to the corresponding intermetallic compounds, Fe_3Al and FeAl, on further milling.

According to them no intermediate phase, i.e., solid solution, was formed during MA as a precursor to the intermetallic phase. The rate of the mechanical alloying process was found to be dependent on milling variables such as rotation speed of mill, ball-to-powder weight ratio and number of milling balls. Liu et al. [38] reported the synthesis of nanostructured B2 intermetallic compounds like NiAl and FeAl by MA of the elemental powder mixtures followed by subsequent heat treatment. They showed that nanocrystalline NiAl, which is difficult to disorder by milling, could be synthesized directly by MA for a particular milling period due to an occurrence of an exothermic explosive reaction. However, FeAl was formed after isothermal annealing of the as-milled powder. Large heat of formation was the main driving force for the formation of NiAl during milling. In case of Fe-Al they reported that during milling a Fe(Al) solid solution was formed by interdiffusion. They reported that the difference in diffusivity in Ni-Al and Fe-Al system was the main cause of the difference in behaviours during the formation of NiAl and FeAl by MA. Nayak et al. [39] reported the mechanical alloying of $Al_{100-x}Fe_x$, (x = 2.5, 5, 10, 15 and 20) alloys. The authors reported that no other phases had formed other than the formation of supersaturated solution of Fe in Al in the case of Al-(2.5-10)% Fe alloys, while in case of Al–20% Fe alloy nanocrystalline metastable Al_5Fe_2 phase was formed. They also reported that during MA an intermetallic phase was formed only when the crystallite size dropped below a critical value of 20 nm. Nanocomposite of α-Al and nanocrystalline intermetallics like Al_6Fe, Al_5Fe_2 and $Al_{13}Fe_4$ in the alloy was formed after annealing at a temperature above 673 K, which was identified as the peak ageing temperature for the nanocrystalline Al-Fe alloys. Huang et al. [40] reported on the formation of metastable phases during mechanical alloying of the Al-Fe binary system. They reported that for Al-rich (up to 10 at. % Fe) alloys, the supersaturated FCC solid solution of Fe in Al (upto 1 at. % Fe) was formed. However, almost complete amorphization was confirmed in the composition range of Al-(17-33) at. % Fe. They reported that metastable disordered BCC solid solution having a grain size of about 10 nm was formed after milling in Fe-rich (above 50 at.% Fe) alloys. The effects of milling intensity on the amorphization of Al-Fe powder mixtures containing 10, 15, 20 and 25 at. % Fe, during MA was investigated by Zou et al. [41]. Two levels of milling intensity, 80*g* and 150*g* (where *g* is acceleration due to gravity) was adopted by them. They reported that two different path ways of amorphization reaction could be observed. One path way was found to be, Al-Fe solid solution → amorphous phase. While the other path was found to be Al-Fe solid solution → formation of Al_5Fe_2 phase → amorphous phase. The first reaction was observed in the case of Al-10, 15, 20 and 25 at. % Fe compositions at lower milling intensity and in Al-10 at. % Fe at higher milling intensity. The latter reaction was observed in Al-15, 20 and 25 at. % Fe compositions at the higher milling intensity. The authors also reported that the amorphization time is strongly dependent on higher milling intensity due to two main reasons. Firstly, higher milling intensity led to an increase in the rate of cold welding and fracturing of the particles. This in turn resulted in the rise of the density of Al-Fe interfaces. This also led to the rapid increase in the rate of interdiffusion between the Al and Fe atoms. Secondly, the high collision pressure led to the high rate of interdiffusion between the Al and Fe atoms.

Adabavazeh et al. [42] reported the synthesis of intermetallic compound having composition of $Ni_{50}Fe_{25}Al_{25}$ by MA of elemental powder mixtures of Ni, Fe and Al. The authors reported in the literature about the effect of substitution of Fe atoms in Ni_3Al alloy during MA and on the final product. According to their paper during the early stages of milling Ni (Al, Fe) solid solution having a layered nanocrystalline structure consisting of cold welded Ni, Al and Fe layers could be observed. During the later stages of milling, this structure transformed to the disordered $(Ni, Fe)_3Al$ intermetallic compound which increased the degree of $L1_2$ ordering upon heating. In comparison to Ni-Al system, Ni (Al, Fe) solid solution formed after a longer period of milling. The substitution of Fe in Ni_3Al alloy delayed the formation of Ni (Al, Fe) solid solution and $(Ni, Fe)_3Al$ intermetallic compound. Krasnowski et al. [43] investigated the phase development during mechanical alloying of Fe-50 at. % Al powder mixture and the subsequent heating of the milled powder. From their work they concluded that the Fe(Al) solid solution is formed not by the gradual diffusion of Al into BCC Fe but by the rapid formation of Fe(Al) coexisting with other phases. During the initial stages of milling very small regions appear in which the Al atoms are dissolved in Fe lattice, creating primary BCC Fe(Al) solid solution zones. At this stage of milling three phases, namely, Fe, Fe(Al) and Al coexist in the milled powder. With increasing milling time all Al atoms dissolve in the Fe lattice. The disordered Fe(Al) solid solution transformed into the ordered FeAl intermetallic compound on annealing. Bonetti et al. [44, 45] reported on the MA behavior of $Fe_{75}Al_{25}$ powder mixture in a high energy ball mill. They reported the extended solid solution of Al in Fe after 1 h of milling and no amorphization reaction occurred even after 32 h of MA. Thermal analysis of the milled powder showed that Fe(Al) solid solution transformed to the ordered Fe_3Al and FeAl intermetallic compounds.

2.5 Fe_3Al Intermetallic Compound as Reinforcement in MMCs

Fe_3Al can be used as reinforcement in various MMCs due to its better bonding and compatibility with the metal matrix. Very few research papers are available in the literature on the use of Fe_3Al as reinforcement in MMCs. Tu et al. [46] has reported on the friction and wear behavior of Cu-Fe_3Al composites developed by powder metallurgy route. They analyzed the effects of contact pressure and sliding speed on the wear behaviour of Cu-Fe_3Al composites. According to them at low contact pressures, wear resistance of the composites increased with the increase in volume fraction of Fe_3Al particulates. At high contact pressures, due to the poor interfacial bonding between the particles and the matrix, a critical volume fraction of Fe_3Al particulate which depended mainly on the contact pressure, was observed. With increasing volume fraction of the reinforcement, the wear resistance increased upto the critical volume fraction. However, the wear resistance showed a decrease beyond the critical volume fraction of the reinforcement. They also reported that the coefficient of friction for the composites was lower than that for the unreinforced matrix alloy and decreased with increase in volume fraction of Fe_3Al. Venkateswaran et al. [47] reported about the dry sliding wear behavior of Cu-based MMCs reinforced with the Fe_3Al intermetallic particulates developed by powder metallurgy route. They had shown that the wear rate of unreinforced alloy (Cu-90%, Sn-10%) was more than that of composite material. With the increase in volume percentage of Fe_3Al in the Cu-Sn matrix the wear rate of the composite decreased. They concluded that Fe_3Al particles had a significant effect on the wear behavior of the composite by providing better support to the metal matrix. Velasco et al. [48] reported on the mechanical properties and wear behaviour of Al-based MMCs where Fe_3Al intermetallic compound was used as reinforcement. They had used three different Fe_3Al intermetallics developed by mechanical alloying for different periods of time to produce Al-based MMCs reinforced with Fe_3Al intermetallic compound. Two reinforcements reported by them were, 5 h and 20 h mechanically alloyed powder, whereas the third was the 20 h mechanically alloyed powder heat treated at 1000 ^oC.

● ● ● ● ● ●

Chapter 3

Experimental Procedure

3.1 Introduction

This chapter is devoted to the experimental techniques which have been adopted in the present research work. The various equipments/instruments which have been used to carry out the experiments are listed in this chapter along with their specifications and particulars. Figure 3.1 shows the work plan that has been adopted.

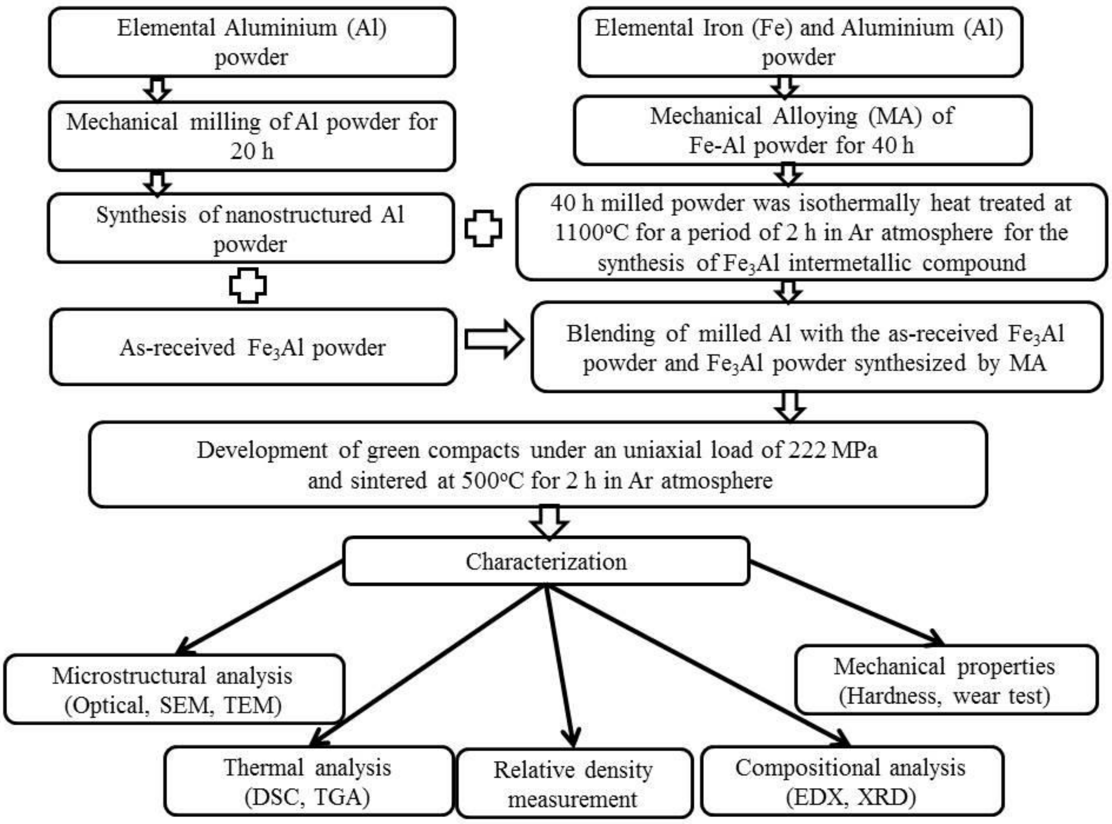

Figure 3.1: Methodology for the present research

In our present investigation, Al powder having purity > 99.99 % was procured from Loba Chemie. Al was milled in a high energy Fritsch P5 planetary ball mill for a period of 20 h in wet medium using toluene as the process controlling agent. For the synthesis of Fe_3Al intermetallic compound by mechanical alloying (MA), elemental Fe and Al powders were taken in a proper stoichiometric ratio and were milled for a period of 40 h. the milled powder was taken out intermittently from the vial after fixed intervals of milling period. These samples were characterized by using x-ray diffraction (XRD), scanning electron microscope (SEM), energy dispersive x-ray analysis (EDX), high resolution transmission electron microscope (HRTEM) and differential scanning calorimetry/thermogravimetric analysis (DSC/TGA). Thermal analysis of the mechanically alloyed Fe_3Al powder was done to in order to precisely determine the temperature of phase transformation from the disordered state to the ordered state. Al-based metal matrix composites were developed by powder metallurgy route by using both as-received Fe_3Al powder and Fe_3Al powder synthesized by MA of $Fe_{75}Al_{25}$ powder followed by subsequent annealing of the milled powder as reinforcement. Al-10, 20, 30 vol. % Fe_3Al composites were developed by cold compaction of the blended powder under a uniaxial compressive load of 222 MPa followed by sintering at 500 ^oC for 2 h in Ar atmosphere. The morphology of sintered samples was characterized by using optical microscopy and SEM equipped with EDX. Hardness of the various sintered samples was determined by Vickers microhardness tester using a diamond indenter. Dry sliding wear test was carried out using a ball-on-plate tribometer having a diamond indenter. Densities of the samples were measured by Archimedes' principle.

3.2 Test Methodology/ Equipments Used in the Present Research Work

3.2.1 High Energy Planetary Ball Mill

In the present research work, a Fritsch P5 high energy planetary ball mill has been used to develop nanostructured Al powder and for the synthesis of Fe_3Al intermetallic compound by the milling of elemental Al and Fe in a proper stoichiometric ratio. The as-milled nanocrystalline Al powder was later used for the development of Al-based metal matrix composites. During high-energy ball milling, the powder particles are repeatedly flattened, cold welded, work hardened, fractured and rewelded. Whenever the balls collide there is always some amount of powder particles that get trapped between the balls. Initially the particles have strong affinity to weld together due to their soft nature resulting in formation of larger particle. With continued deformation, the force resulting from the impact of the balls plastically deforms the powder particles leading to work hardening and fracture. With continued deformation, the particles get work hardened thus resulting in fracture by fatigue failure mechanism, i.e., by the fragmentation of fragile flakes. Fragments generated by this mechanism may continue to reduce in size in the absence of strong agglomerating forces.

In high energy planetary ball mill there is a specially designed circular disc on which the vials are placed. The disc and the vials rotate in opposite direction with respect to each other. This rotation of the disc and vials provides centrifugal force to the balls. The centrifugal force helps in transferring the necessary and sufficient energy to the powder particles by the impact of the balls. The speed at which the powders get reduced to nanometric dimension is very close to the critical speed. Beyond the critical speed the balls get pinned to the inner walls of the vials due to the dominance of the centrifugal force over the centripetal force and do not exert any impact on the powder and thus causing no further grinding. However, below the critical speed the higher the milling speed, the higher is the milling intensity. During the process of milling the crystallite size of the milled powder can be brought down to nanometric dimension. As the particle size goes on decreasing, the chance of agglomeration increases simultaneously due to higher surface energy of nanosized particles. In order to avoid agglomeration of the nanoparticles, a process controlling agent (PCA) is used. In the present work, toluene has been used as the process controlling agent. The PCA gets adsorbed on the surface of the powder particles and forms a thin layer surrounding the particle. This thin layer precludes the possibility of particle agglomeration and also minimizes cold welding. At this stage, the tendency to fracture predominates over cold welding.

Intermetallics are one of the most promising materials for high temperature applications. They are usually produced by solid state reactive synthesis. The formation of intermetallics is the result of an exothermic reaction thus involving a release of high amount of heat energy. Hence, it is difficult to produce intermetallics by conventional techniques. However, mechanical alloying (MA) has been found to be a highly suitable and economically viable technique for the synthesis of intermetallics. Here, in this research work, elemental Fe and Al powders were blended in a proper stoichiometric ratio and milled for upto 40 h in order to synthesize iron aluminide (Fe_3Al) intermetallic compound. Also in this work, Al powder was milled upto 20 h in order to synthesize nanostructured Al powder. The nanostructured Al powder was later used for the development of the various Al-Fe_3Al composites.
The milling conditions adopted in the present research work are:

Milling Parameters

- Type of mill : Fritsch P5 planetary ball mill
- Milling media: Both the vials and balls are made of hardened chrome steel

- Milling speed : 300 rpm
- Milling time : up to 20 h for the synthesis of nanostructured Al and upto 40 h for the synthesis of intermetallic Fe_3Al compound
- Ball diameter: 10 mm
- Ball-to-powder weight ratio: 10:1
- Milling medium: Wet (toluene is used as process controlling agent)
- Temperature of milling (room temperature)

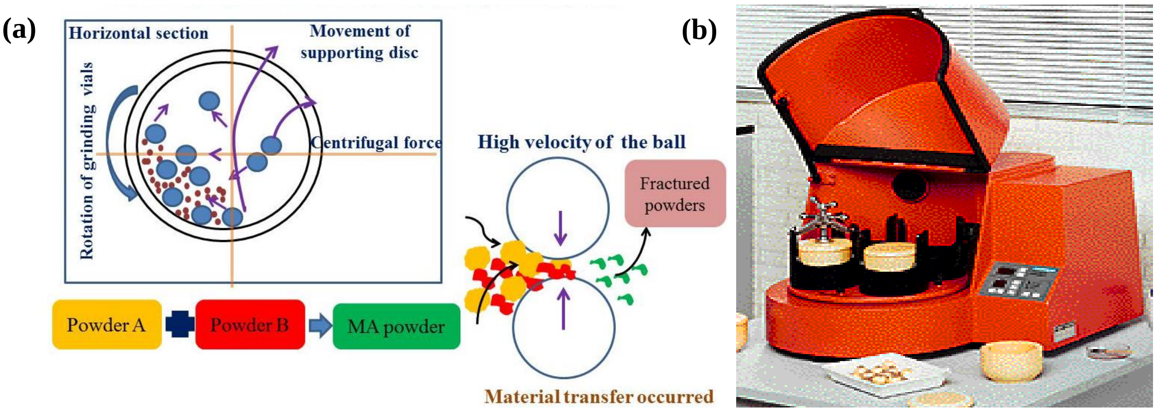

Figure 3.2: (a) Schematic representation of the mechanical alloying process (b) Fritsch P5 planetary high energy ball mill

3.2.2 Uniaxial Hydraulic Press

Uniaxial die pressing is one of the most popular and economically viable technique that is used to manufacture near net shape products. In this machine, powder particles are compacted inside the die by the application of a load through the punch. It is used for making the green samples which are later sintered in a furnace. The load is applied from only one direction and this is why it is named as uniaxial hydraulic press. Two punches or piston have been used here. Among them the bigger punch is movable whereas the smaller one remains steady. The presses used are generally mechanical or hydraulic. Here in the present research work, a cold uniaxial hydraulic press has been used using a 15 mm die for the compaction and development of green samples. The uniaxial cold compaction of all the samples was done under a load of 222 MPa. The above specifications were applied to all the samples developed in the present research work. The uniaxial hydraulic press used was designed by Soillab with maximum capacity of 1130 MPa.

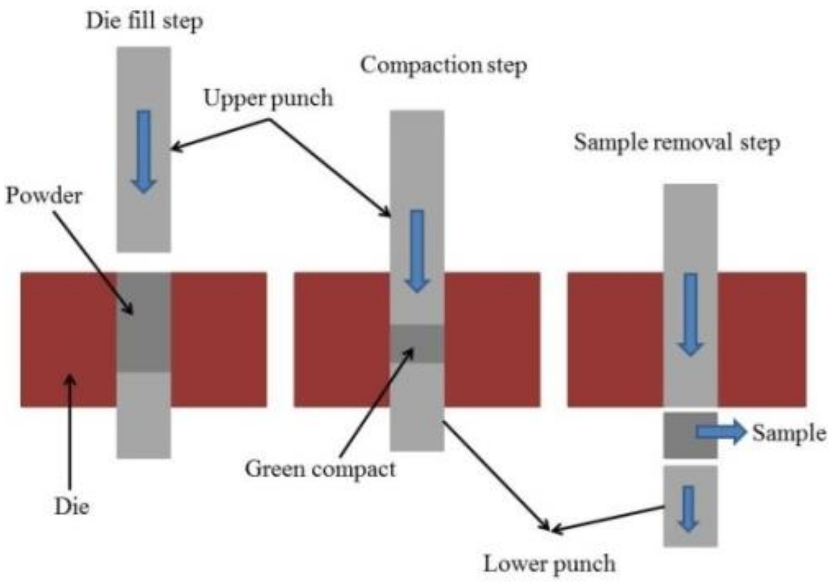

Figure 3.3: Schematic representation of the uniaxial hydraulic press

3.2.3 X-ray Diffraction

A diffractometer is an instrument used for analyzing the structure of a material from the scattering pattern created when a beam of radiation or particles (such as x-rays or neutrons) interact with it. An x-ray diffractometer illuminates a sample with x-rays of known wavelength by moving the sample and detector in order to measure the intensity of the diffracted radiation as a function of beam and sample orientation. X-ray diffraction (XRD) is extensively used in areas such as qualitative and quantitative phase analysis, crystallography, structure determination, texture, crystallite size, lattice parameter and residual stress investigations. From the resulting intensity versus angle plot much can be inferred about the structure of the material. In the present research work, x-ray diffraction of the milled powder has been carried out in order to analyze the crystallite size, lattice parameter, and residual strain of the milled powder after different intervals of milling periods. For this purpose the milled powder was taken out after different intervals of milling period. In this research work, XRD technique has been used to confirm the synthesis of nanostructured Al and the formation of Fe_3Al intermetallic compound synthesized by mechanical alloying of elemental powder mixtures of Fe and Al in a proper stoichiometric ratio. The various Al-Fe_3Al composites were also analyzed by XRD technique to detect the formation of any new phase that may have been formed during the development of the composites. X-ray diffraction of the various samples were done in a Phillips PANalytical diffractometer using Cu Kα radiation (λ = 1.5409 Å), where Ni was used as filter.

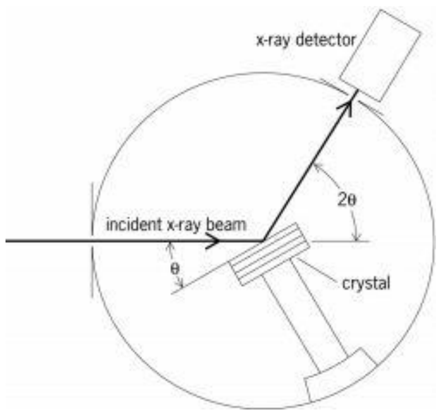

Figure 3.4: Schematic representation of the x-ray diffractometer

3.2.4 High Temperature Tubular Furnace

The high temperature tubular furnace is one of the most popular electric heating devices. It is used widely for sintering of green compacts. The design comprises of a cylindrical cavity surrounded by heating coils that are rooted in a thermally insulating matrix. The temperature of the furnace can be controlled by response from a thermocouple. The furnace comprises of insulation plugs and gas tight end seals in order to prevent any kind of heat loss. In our present investigation, green compacts developed via uniaxial compaction were heated up to 500 ^{o}C for 2 h in the presence of Ar atmosphere. The samples are heated in a crucible in an inert atmosphere of argon gas. The design of the furnace ensures uniform heating of the green compacts that enhances the bonding strength between the powder particles. A vacuum and controlled atmosphere furnace manufactured by Naskar & Company with maximum attainable temperature of 1750 ^{o}C was used for the present investigation.

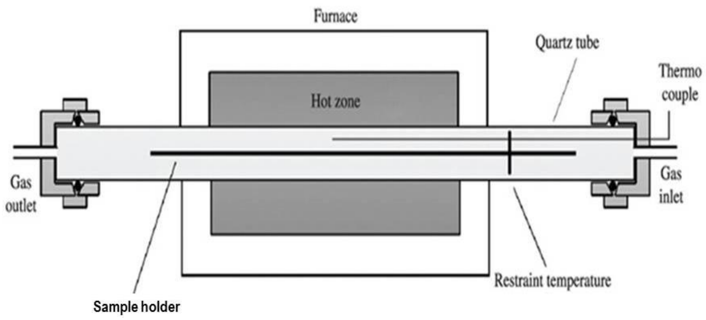

Figure 3.5: Schematic representation of a high temperature tubular furnace

3.2.5 Scanning Electron Microscopy (SEM)

In a scanning electron microscope (SEM) an electron beam is generated by a suitable source, typically a tungsten filament or a field emission gun. This electron beam is then accelerated by applying a high voltage and is made to pass through a system of apertures and electromagnetic lenses to produce a thin beam of electrons. The electron beam is concentrated to a fine probe to produce images. The focused beam of high-energy electrons scans the polished surface of the sample and produces a raster like pattern. When the electrons strike the sample, it emits signals in the form of electromagnetic radiation which are then collected by suitably-positioned detectors. The signals that are derived from the electron-sample interactions are collected by detectors and reveal information about the sample including morphology, chemical composition, and crystalline structure. These signals include secondary electrons (SE), backscattered electrons (BSE), Auger electrons, characteristic x-rays etc. The secondary electrons (SE) and the backscattered electrons (BSE) are mainly used for imaging. Imaging using the secondary electrons provides information about the morphology and the surface topography whereas the backscattered electrons are used for illustrating contrasts in composition in multiphase samples. The signals are amplified and displayed on a monitor. SEM produces an image of magnification equivalent to the ratio of the size of the screen to the size of area scanned on the sample. The SEM is also capable of performing analysis of selected point locations on the sample. The energy-dispersive x-ray (EDX) analysis permits the operator to determine the composition and spatial distribution of elements in a sample. The three principal components of a basic EDX system are the x-ray detector, the pulse processor that measures the voltage pulses that are analogous to the x-ray energies and computer. Element maps are extremely beneficial in finding out the elemental distribution in a sample. The elemental maps principally show the compositional variation. In the present research work, a JEOL-JSM-6480LV SEM has been used. It is equipped with an INCA Penta FET-x3 x-ray microanalysis system with a high-angle ultra-thin window detector and a 30 mm^2 lithium-drifted silicon detector crystal was used. Various powder samples like milled Al powder, as-received Fe_3Al powder, Fe_3Al synthesized by MA and sintered pure Al and various Al-Fe_3Al composite samples were characterized using SEM. The operating voltage of the SEM was 20 kV and the secondary electron imaging mode has been used.

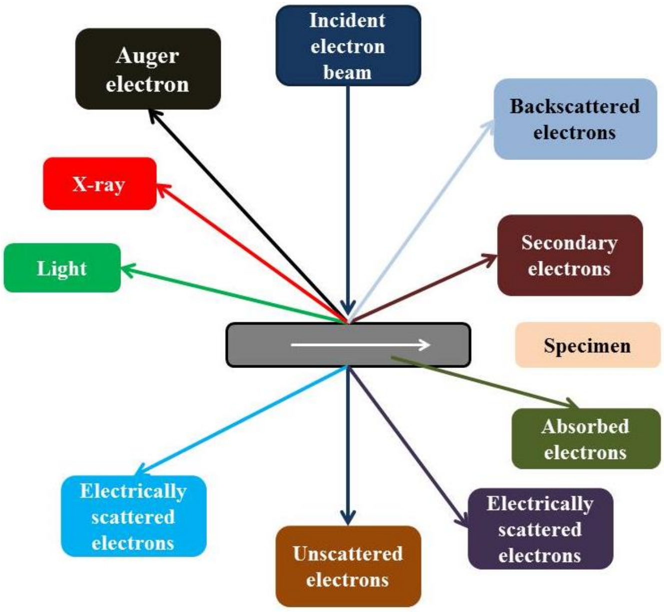

Figure 3.6: Schematic representation of the specimen-beam interaction in a SEM

3.2.6 High Resolution Transmission Electron Microscopy (HRTEM)

High resolution transmission electron microscopy (HRTEM) is a technique that uses electron beams which are transmitted through thin specimens and it interacts with the specimen as it passes through it. From the interaction of the electrons transmitted through the specimen an image is formed. A beam of electrons from the electron gun is focused into a small, thin, coherent beam by the condenser lens. This beam is restricted by the condenser aperture, which excludes high angle electrons. The beam then strikes the specimen and part of it is transmitted depending upon the thickness and electron transparency of the specimen. This transmitted portion is focused by the objective lens into an image on a phosphor screen or charge coupled device (CCD) camera. The basic principle behind the working of HRTEM is the diffraction of electron beam by the periodically arranged atoms inside the samples. The images and diffraction patterns formed using a TEM reveal the information about the crystal structure of the sample being investigated. In the present research work a JEOL JEM-2100 HRTEM with a point to point resolution of 0.194 nm was used to analyze the 20 h milled nanostructured Al powder and the Fe_3Al powder developed by mechanical alloying. The operating voltage of the HRTEM was 200 keV. The powder samples were dispersed in acetone solution by ultrasonication. The powder dispersed in acetone solution was put on a carbon coated copper grid to observe the samples in the HRTEM. Selected area diffraction (SAD) pattern of all the samples have also been taken using the HRTEM.

3.2.7 Vickers Microhardness

Vickers microhardness is one of the most widely used methods for determining the hardness of metallic samples. In the present research work, this hardness determination technique has been used for determining the hardness of the various sintered pure metals and metal matrix composite samples. The Vickers hardness tester uses a square based pyramid diamond indenter having an angle of 136^o between the opposite faces. Based on the shape of the indenter, it is also popularly known as diamond pyramid hardness (DPH) tester. The unit of hardness given by the test is known as the Vickers Pyramid Number (HV) or Diamond Pyramid Hardness (DPH).

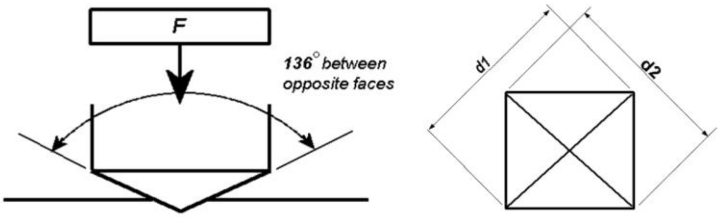

Figure 3.7: Schematic representation of Vickers microhardness tester

The Vickers hardness is the quotient obtained by dividing the load by the area of indentation and can be expressed as given below.

$$\boldsymbol{HV = \frac{2p\sin\frac{\theta}{2}}{L^2} = \frac{1.854P}{L^2}} \quad \dots (1)$$

$$\mathbf{L = \frac{d1 + d2}{2}} \quad \dots (\mathbf{2})$$

Where,
P= applied load (kgf)
L= average length of diagonals, (d1+d2)/2, (mm)
θ= angle between opposite faces of the diamond indenter (136^o)

Here, the two diagonals d1 and d2 of the indentation left on the surface of the material after removal of the load are measured and their arithmetic mean L is calculated from the above formula. Vickers hardness number is defined as load applied divided by the surface area of the indentation. This area can be calculated from the measurement of the lengths of diagonals of the indentation. In our research load of 100 gf was used for a dwell time of 10 sec. In the present investigation the microhardness measurements were done using a Lecco Vickers microhardness tester (LV 700) using a diamond indenter.

3.2.8 Density Measurement

The density of the various samples was determined using Archimedes' principle. It is very difficult to measure the accurate density of sintered samples as there are several errors in density measurement owing to the presence of interconnected and disconnected pores in the samples. Liquid gets into the interconnected pore and affects the density measurement. In order to minimize this error, three weight measurements were taken, weight in air or dry weight (W_{air}), weight of the sample dipped in liquid or dipped weight (W_{liquid}), and weight of the sample in air after soaking in liquid for a long time or soaked weight (W_{soaked}). The liquid used is distilled water (ρ_{liquid} =1.0 gm/cc). Density of the sample is determined form the three weights taken for each sample using the following formula.

$$\rho_c = W_{air} \text{ x } \rho_{liquid}/(W_{soaked} - W_{liquid}) \quad \dots (1)$$

Where,

- ρ_c = Density of the composite, gm/cc
- Weight of the sample in air W_1=W_{air}, gm
- Weight of the sample in liquid W_2 = W_{liquid}, gm
- Weight of the sample soaked in liquid for a long time W_3 = W_{soaked}, gm

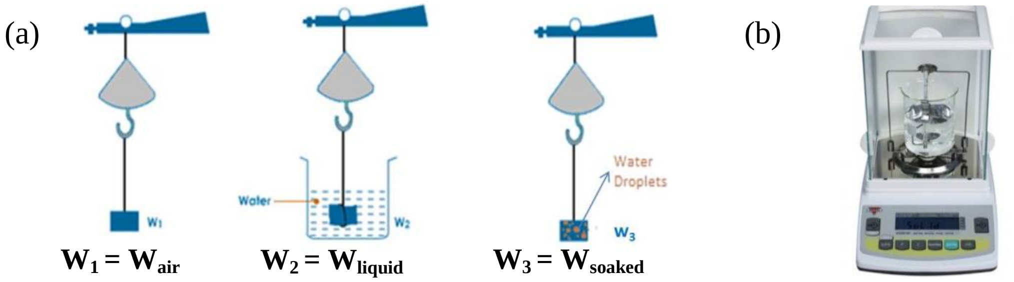

Figure 3.8: (a) Experimental setup for density measurement (b) Density measurement kit

3.2.9 Wear Test

Wear is a process of removal of material from one or both of two solid surfaces as a result of relative motion between these two solid surfaces. It is basically the erosion of the material from its base position on a solid surface. Wear is linked to the interactions between two surfaces. Specifically it is the removal and deformation of material on a surface due to the mechanical action of the opposite surfaces. The relative motion between the two surfaces and the initial mechanical contact between asperities are one of the important factors in wear. Wear test is carried out to find the wear characteristics of the composites developed by powder metallurgy route and to understand the wear mechanism. A computerized ball-on-plate wear tester (TR-208-M1, DUCOM) equipped with a diamond indenter was used for dry sliding wear test. Wear test prerequisites including sample surface polishing and cleaning were carried out. The wear test was conducted at a rotational sliding speed of 20 rpm under a load of 20 N for a period of 10 minutes for all sintered samples. The worn surfaces of these samples were characterized using SEM to identify the wear mechanism. The width of wear tracks was also measured.

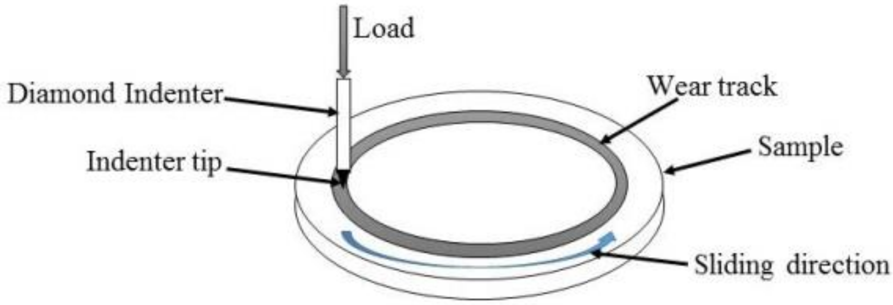

Figure 3.9: Schematic diagram of wear tester

3.2.10 Thermal Analysis

Differential scanning calorimetry and thermogravimetric analysis (DSC/TGA) was done in a NETZSCH STA 409C simultaneous thermal analyzer at a heating rate of 10^{o}C/min in the temperature range of 50 to 1000 ^{o}C in Ar atmosphere in order to determine thermal stability of the various samples.

• • • • •

Chapter 4

Results and Discussion

4.1 Introduction

Aluminium based metal matrix composites (MMC) have gained considerable attention as structural materials in various areas like aerospace, automotive and transportation industries because of their high specific modulus, specific strength and superior fatigue and creep resistance. The present work investigates the microstructure, dry sliding wear resistance and hardness of Al-based MMCs developed by powder metallurgy route reinforced with different vol. % of Fe_3Al intermetallic compound. In the next four sections of this chapter, 'Mechanical Milling (MM) of Al', 'Development of Al-Fe_3Al Composites by Powder Metallurgy Route using as-received Fe_3Al as Reinforcement', 'Synthesis of Fe_3Al Intermetallic Compound by Mechanical Alloying (MA)' and 'Development of Al-Fe_3Al Composites by Powder Metallurgy Route using Fe_3Al Synthesized by MA' has been discussed.

4.2 Mechanical Milling (MM) of Al

Mechanical milling (MM) is a solid state size reduction process where the material charged in the form of coarse particles are broken into bulk fine powder by the mechanical impact created due to the collision between the charged powder with the milling media. MM is the milling of uniform composition powders such as pure metal powders or pre-alloyed powders, where material transfer is not necessary for homogenization. During mechanical milling, the charged material is placed together with the milling balls in a vial. High rotational speed of the supporting disc and the vial produces high travelling speed of the charged material and milling media leading to high impact energy. The energy generated during the impact leads to fracture of the charged material into smaller sizes. In our present research work elemental Al powder was milled for a period of 20 h in order to synthesize nanostructured Al powder. Al was milled in a Fritsch pulverisette P5 high energy planetary ball mill for a period of 20 h in wet medium using toluene as the process controlling agent. Samples of milled Al were collected at regular intervals of 5 h. The x-ray diffraction plots of Al milled for various periods of milling time is shown in Figure 4.1 (a). No peaks due to the contamination from milling media could be found in the x-ray diffraction plots. Figure 4.1 (b) shows the variation of crystallite size of Al with milling time. Al shows a gradual decrease in crystallite size with milling time up to 15 h of milling. Beyond 15 h of milling there was a slight rise in crystallite size possibly due to cold welding taking place during milling. The crystallite size of Al after 20 h of milling was found to be 54 nm. Al is very ductile and this is why it is not possible to reduce its crystallite size to a very low value even after 20 h of milling. Figure 4.1 (c) shows the variation of strain with milling time for Al. There is a gradual increase in r.m.s. strain with increase in milling time. Precise lattice parameter was calculated using the Nelson-Riley parameter. Figure 4.1 (d) shows the variation of lattice parameter with milling time for Al. Lattice parameter of Al shows slight decrease up to 15 h of milling but beyond 15 h of milling its shows an increase [49].

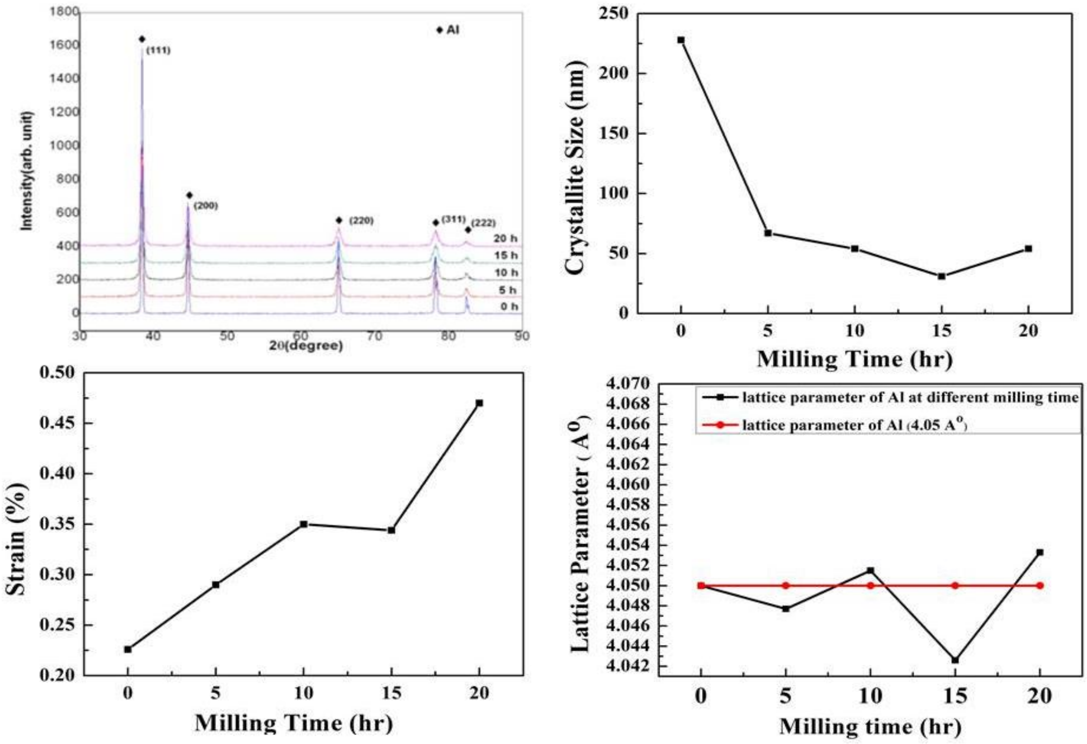

Figure 4.1: (a) X-ray diffraction of Al milled for various periods of time. Variation of (b) crystallite size (c) strain (d) lattice parameter of Al with milling time

Table 4.1: XRD analysis of 20 h milled Al powder

Milling Time (hr)	Crystallite Size (nm)	Strain (%)	Lattice Parameter (Å)
0	228	0.226	4.05
5	67	0.29	4.0477
10	54	0.35	4.0515
15	31	0.344	4.0426
20	54	0.47	4.0533

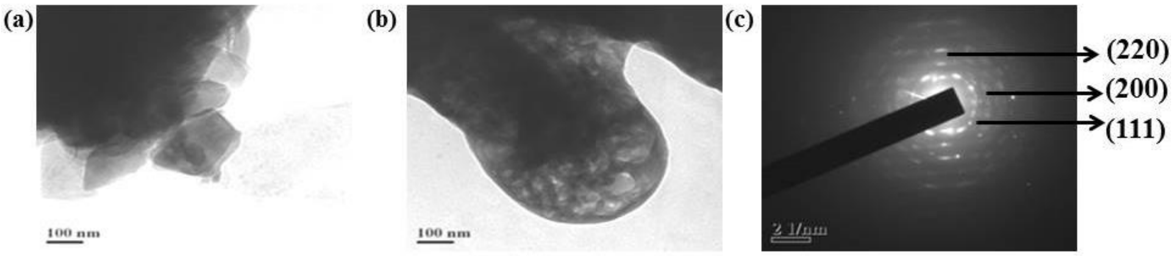

Figure 4.2: (a, b) HRTEM images (c) SAD pattern of 20 h milled Al powder

The HRTEM images in Figures 4.2 (a, b) show that the 20 h milled Al powder is nanometric in dimension. It is evident from the HRTEM images that cold welding of the milled Al has taken place. The ring pattern of the SAD image also indicates in Figure 4.2 (c) that the 20 h milled Al powder is nanometric in dimension. The rings in the SAD pattern could be indexed to the (111), (200) and (220) planes of the Al lattice.

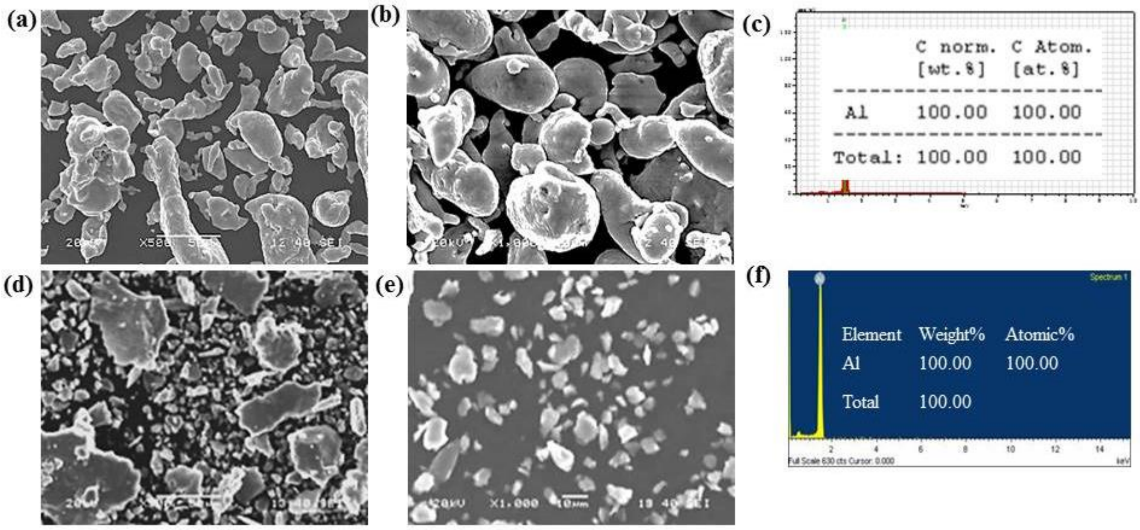

Figure 4.3: (a, b) SEM images of as-received Al (c) EDX of as-received Al (d, e) SEM images of 20 h milled Al (f) EDX of 20 h milled Al

Figures 4.3 (a, b) show the SEM images of as-received Al powder. Most of the powder particles were found to be nearly spherical. Few particles were also found to be dumbbell shaped or granular. Particles ranging from less than 10 µm to about 30 µm in size could be found in the SEM image of the as-received Al powder. Figure 4.3 (c) is the EDX analysis of the as-received Al. It shows the composition of the as-received powder as 100 % Al. Figures 4.3 (d, e) show the SEM images of Al milled for 20 h. Milling of Al for 20 h leads to a layer type structure. The SEM images also suggest that cold welding between the Al particles have taken place during milling. Large particles having flat surfaces could be seen in the SEM images. Al due to its ductile nature has been flattened during milling. The EDX analysis in Figure 4.3 (f) shows 100 % Al after 20 h of milling. There was no contamination from the milling media. Al is a ductile and soft material and shows very little wear of the vials and balls during milling. Al also does not show any oxidation during milling as Al is known to be highly oxidation resistant. The SEM images in Figures 4.3 (d, e) show the morphology of 20 h milled Al powder. The morphological changes during ball milling of ductile powder like Al can be considered as a combination of two mechanisms, fracture and cold welding. Initially, during milling Al undergo size reduction due to fracturing. Later the ductile Al particles tend to deform and cold weld. The impact of balls during milling flattens the as-received Al particles. These particles later cold weld to form larger disc-shaped particles. Plastic deformation during milling makes the particles hard and brittle and, as a result, fracture mechanism becomes dominant after initial few hours of milling. As a result, the big plate-like particles now fracture to form smaller flake-like particles. During the latter part of milling, fracture mechanism is dominant over cold welding and the flake-like particles change to equiaxed particles and particle size of the powder reduces. This is also evident from the variation of crystallite size with milling time in Figure 4.1 (b) which shows an initial reduction of crystallite size up to 15 h of milling followed by a rise in the crystallite size. It should be noted that within 5 h of milling the rate of reduction in crystallite size is very fast after which the crystallite size reduces gradually up to 15 h [10, 50, 51].

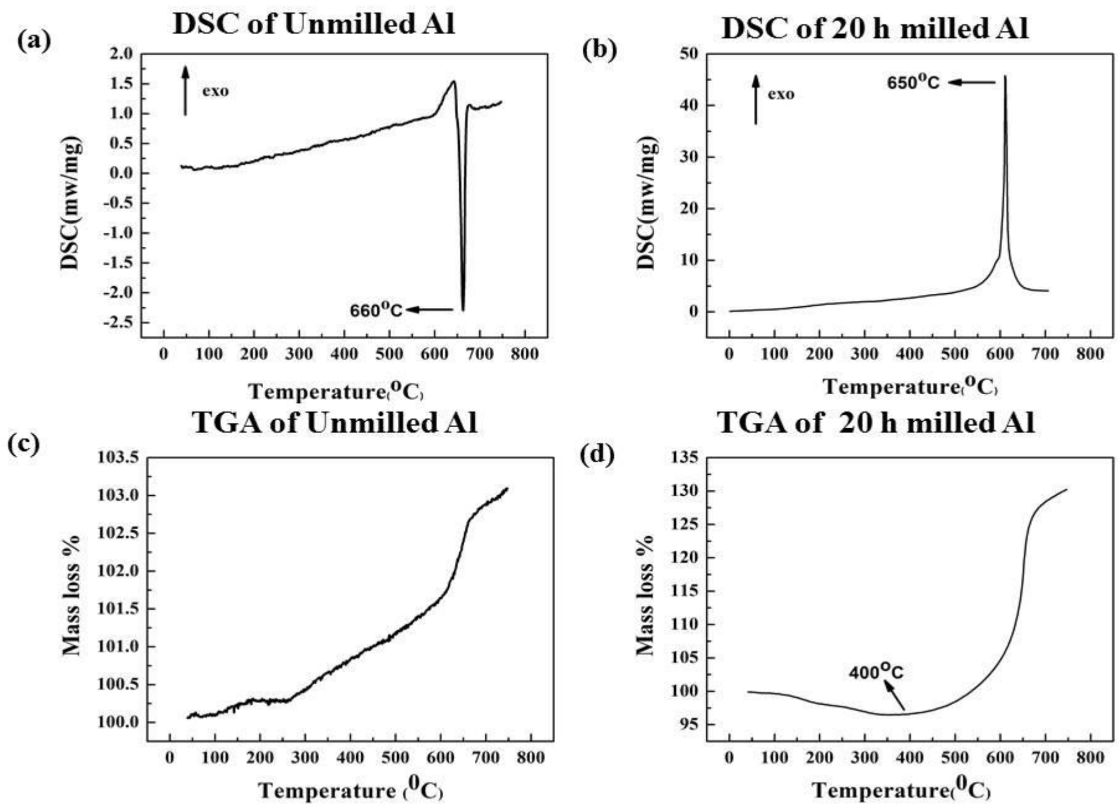

Figure 4.4: (a) DSC (b) TGA of unmilled Al powder and (c) DSC (d) TGA of 20 h milled Al powder

The DSC plot of unmilled Al in Figure 4.4 (a) shows an endothermic peak at around 660 ^{o}C which is the melting point of pure Al (660.2 ^{o}C). On the other hand, the DSC plot of 20 h milled Al in Figure 4.4 (c) shows a sharp exothermic peak at around 650 ^{o}C with the disappearance of the endothermic peak. The exothermic peak here is due to the ordering transition in milled Al. The TGA curve of unmilled Al in Figure 4.4 (b) shows a continuous increase in mass with the rise in temperature. On the other hand the TGA curve of 20 h milled powder in Figure 4.4 (d) shows a slight decrease in mass initially. Milling was done in the wet medium of toluene. The initial decrease in mass was possibly due to the evaporation of residual toluene present in the 20 h milled powder. Toluene was used as the process controlling agent during milling. Beyond 400 ^{o}C there was a continuous rise in mass with the rise in temperature. Comparison of the TGA plots of unmilled and milled Al in Figures 4.4 (b) and (d) respectively show that the increase in mass due to oxidation of Al was very less in the case of unmilled Al but a large increase in mass was seen in the case of 20 h milled Al as it could be oxidized to a higher extent due to the large surface area of the milled powder [52].

4.3 Development of Al-Fe_3Al Composites by Powder Metallurgy Route using as-received Fe_3Al as Reinforcement

Iron aluminide (Fe_3Al) is one of the most popular intermetallic compounds among all aluminides. It has high hardness as well as high wear resistance value. From this point of view it is the most noticeable reinforcement for the development of ductile metal matrix composites. In the present research work 20 h milled nanocrystalline Al powder was used as matrix. Al-Fe_3Al composites have been developed by powder metallurgy route through the following steps.

1. The blending of 20 h milled Al powder and as-received Fe_3Al powder.
2. The green compacts were developed by uniaxial cold compaction under a load of 222 MPa followed by the conventional sintering at 500 ^{o}C for 2 h in Ar atmosphere.
3. The different mechanical properties of the sintered samples were then determined.

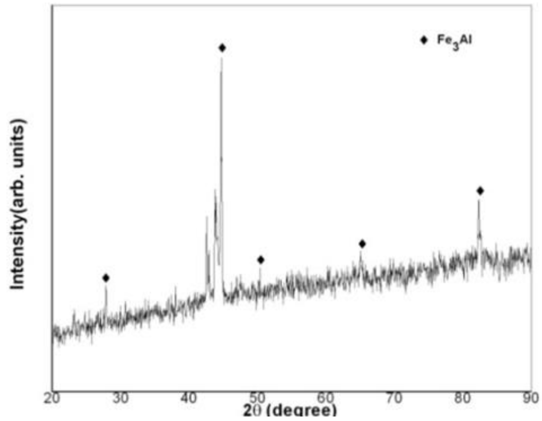

Figure 4.5: X-ray diffraction of as-received Fe_3Al powder

The as-received Fe_3Al powder was characterized by x-ray diffraction using Cu Kα radiation (λ=1.5406 Å). Figure 4.5 shows the x-ray diffraction pattern of as-received Fe_3Al powder. The noticeable peaks which can be seen in the x-ray diffraction plot of Fe_3Al in Figure 4.5 are at 2θ values of 44.1^o, 52^o, 64.2^o, 81.2^o. The various peaks in the XRD plot could be indexed to the (220), (311), (400) and (422) crystallographic planes of Fe_3Al respectively. The appearance of a low-intensity peak at the d-value of 2.89 Å (2θ = 27.8^o) present in the XRD spectrum of the bulk sample, corresponds to the (200) superlattice peak of Fe_3Al. The profile corresponding to the (200) superlattice peak is the direct evidence that the as-received Fe_3Al powder is in ordered state. Ordered Fe_3Al with $D0_3$ crystal structure are considered to be very good structural intermetallic compounds for high temperature applications, due to their excellent high temperature strength and creep resistance [53, 54].

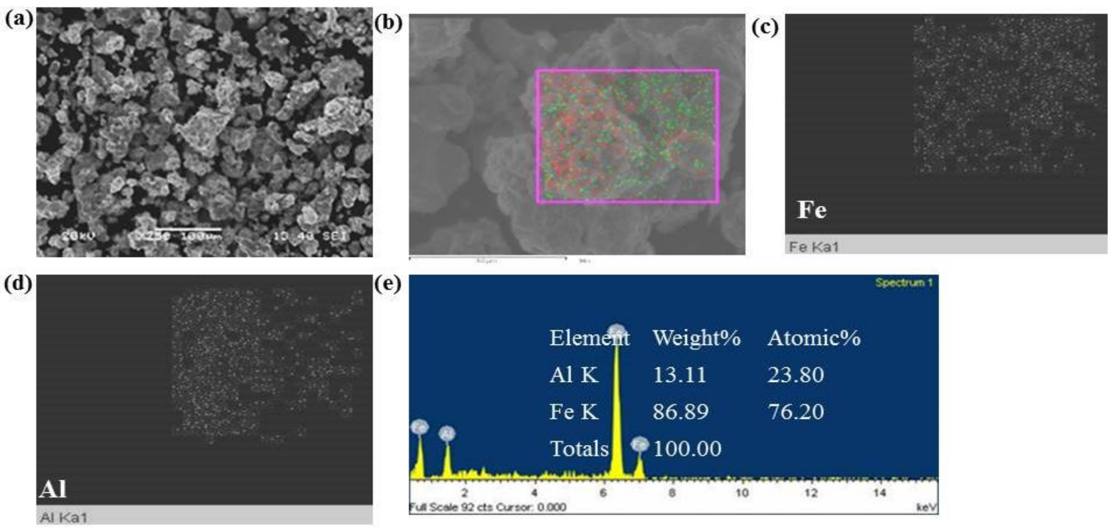

Figure 4.6: (a, b) SEM images of as-received Fe_3Al powder and elemental map of (c) Fe (d) Al in the region shown in the SEM image in (b) and (e) EDX of the sample

Figures 4.6 (a, b) are the SEM images of as-received Fe_3Al powder. The SEM images suggest that the Fe_3Al particles have an irregular morphology. Figures 4.6 (c) and (d) show the elemental maps of Fe and Al respectively in the as-received Fe_3Al powder. Figure 4.6 (b) is the SEM image of the particle used for the elemental maps. The elemental maps of Fe and Al suggest that there is a higher concentration of Fe in the powder. Fe is densely distributed in the powder whereas Al is found to be in slightly lesser concentration. However, it should be noted that both Fe and Al show similar distribution and are found to be present together in the same region. The EDX analysis of as-received Fe_3Al powder in Figure 4.6 (e) shows that the as-received Fe_3Al powder has the composition of Fe (76.20 at. %) and Al (23.80 at. %).

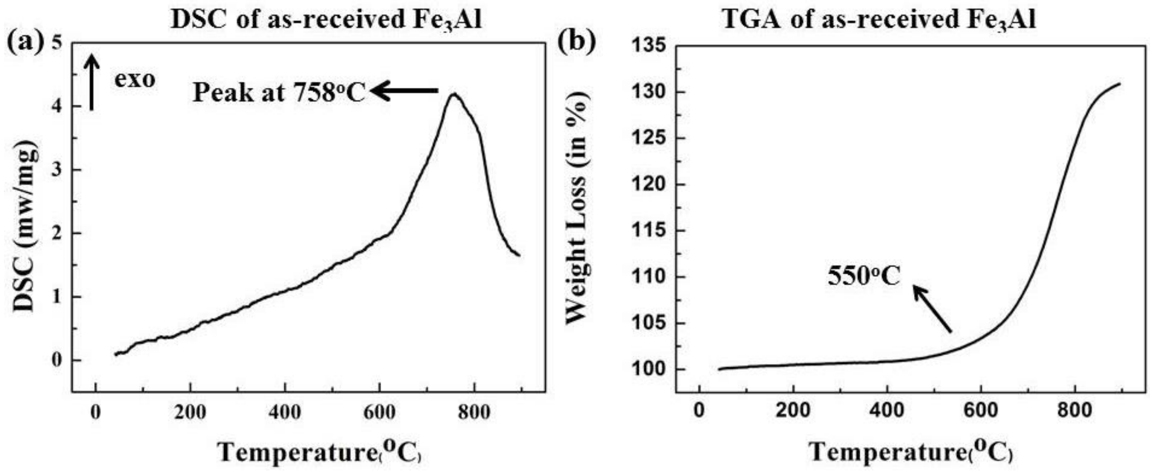

Figure 4.7: (a) DSC (b) TGA of as-received Fe_3Al

The DSC plot in Figure 4.7 (a) suggests that the as-received Fe_3Al powder has high thermal stability. Iron aluminides exhibit order-disorder transformations and large concentrations of defects that depend on temperature and composition. Fe_3Al has ordered cubic $D0_3$ crystal structure. It is known that Fe_3Al transforms from $D0_3$ structure to a defective ordered cubic B2 crystal structure at temperature above the critical ordering temperature of 541 ^{o}C [33]. An exothermic peak at 758 ^{o}C could also be seen in the DSC plot of the as-received Fe_3Al powder shown in Figure 4.7 (a). This peak corresponds to the transformation of Fe_3Al from a $D0_3$ structure to a defective ordered cubic B2 crystal structure ($D0_3 \rightarrow B2$ transition). The TGA plot of as-received Fe_3Al powder in Figure 4.7 (b) shows only a slight oxidation up to the temperature of 550 ^{o}C. A higher weight gain due to oxidation was found in the temperature range of 550 ^{o}C-800 °C. Fe_3Al is known to have very good corrosion resistance [37, 38, 44-46].

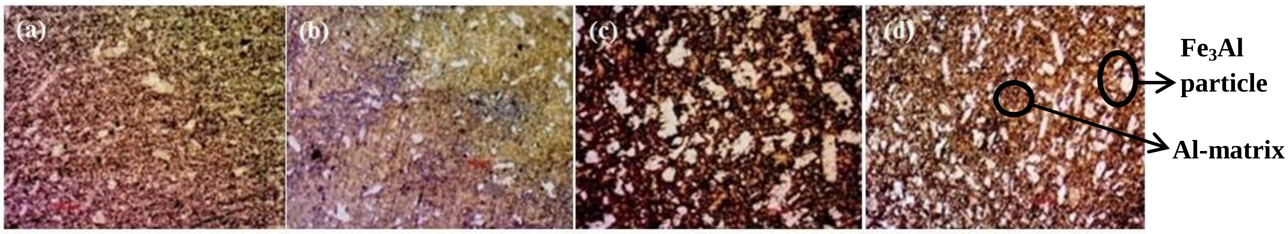

Figure 4.8: Optical images of (a) sintered pure Al (b) Al-10 vol. % Fe_3Al (c) Al-20 vol. % Fe_3Al (d) Al-30 vol. % Fe_3Al sintered composites

Nanocrystalline Al developed by mechanical milling was mixed with different vol. % of Fe_3Al and compacted under a uniaxial load of 222 MPa and sintered at 500 ^oC in Ar atmosphere for 2 h. Figure 4.8 shows the optical micrographs of sintered pure Al and Al-10, 20, 30, vol. % Fe_3Al sintered composites. Figure 4.8 (a) is the optical image of the sintered pure Al sample. The optical images of the various composites in Figures 4.8 (b-d) show light coloured Fe_3Al dispersed homogeneously in the Al matrix. In the optical micrographs of Al-10, 20, 30 vol. % Fe_3Al sintered composites shown in Figure 4.8 (b-d) large Fe_3Al particles having a size in the range of 30-40 µm could be seen in the sintered composites. The Fe_3Al particles are found to be irregular in shape. It can be concluded from the optical micrographs that the Fe_3Al particles are randomly distributed in the Al matrix and agglomeration of Fe_3Al particles in the sintered composites was not observed. The absence of agglomeration of Fe_3Al particles in the Al-Fe_3Al sintered composites can be attributed to the uniform mixing of the powders. The sintered Al-Fe_3Al composites exhibit better homogenous and compact microstructure with the increase of Fe_3Al content in the Al matrix. It can be seen in Figure 4.11 (a) that there is an improvement in the relative density of the Al-Fe_3Al sintered composites with the increase in Fe_3Al content [55-58].

Microstructure characterizations of all the samples have been done using SEM. From the SEM images of Al-10, 20, 30 vol. % Fe_3Al composites in Figure 4.9 large Fe_3Al particles having a size in the range of 30-40 µm could be seen. The EDX analysis of sintered pure Al sample in Figure 4.9 (c) shows the presence of oxygen apart from Al. This is possibly due to the oxidation of Al by the unavoidable oxygen present during sintering. Sintering was done at 500 ^oC for 2 h in Ar atmosphere. The SEM images of Al-10, 20, 30 vol. % Fe_3Al sintered composites in Figures 4.9 (d, i, n) respectively exhibit a homogenous and compact microstructure. The elemental maps of Al and Fe in Al-10, 20, 30 vol. % Fe_3Al sintered composites suggest that the Fe_3Al particles are surrounded by finer Al particles.

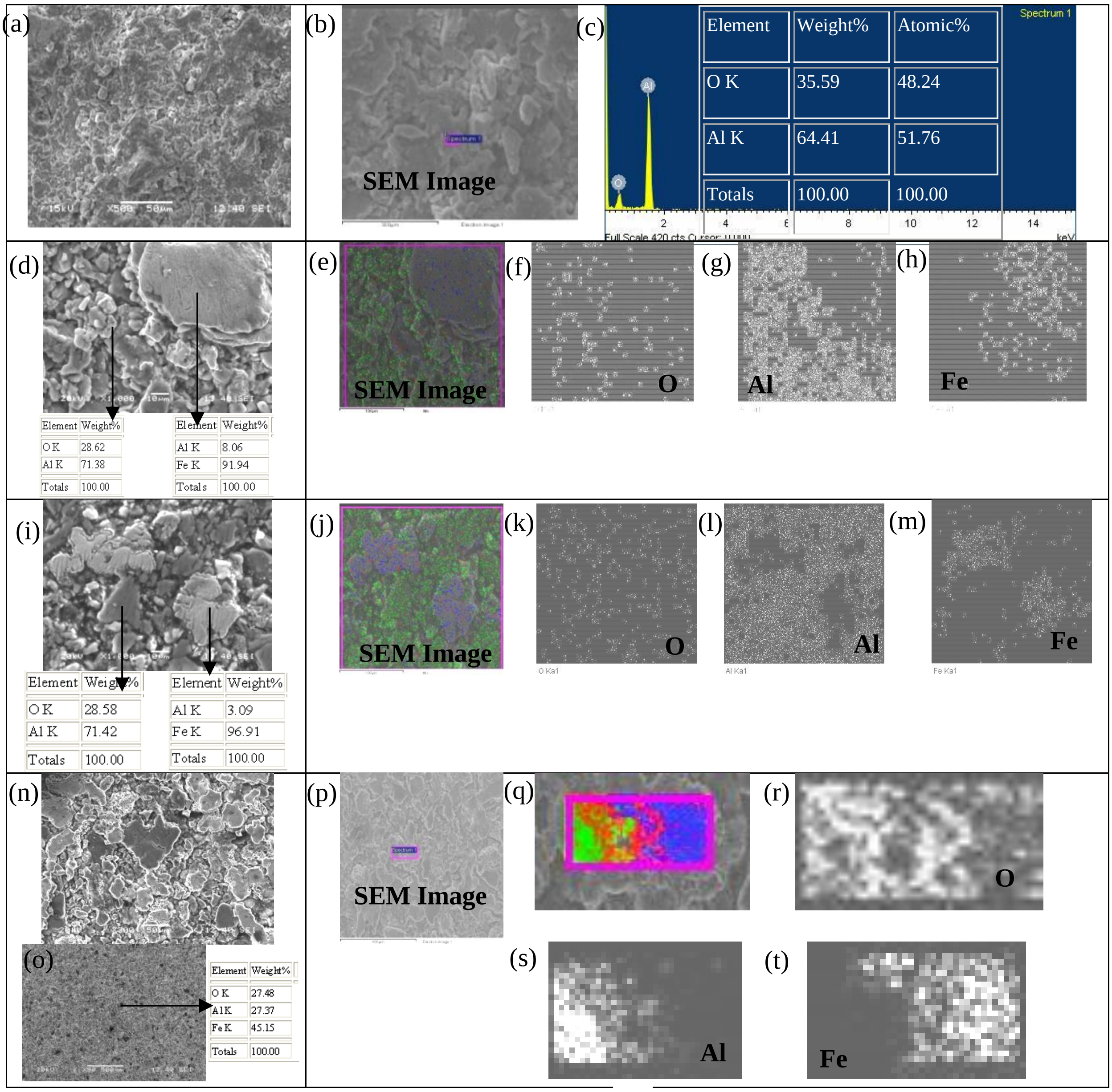

Figure 4.9: (a-c) SEM images and EDX of pure sintered Al. SEM images and an elemental map of O, Al and Fe in (d-h) Al-10 vol. % Fe_3Al (i-m) Al-20 vol. % Fe_3Al and (n-t) Al-30 vol. % Fe_3Al sintered composites

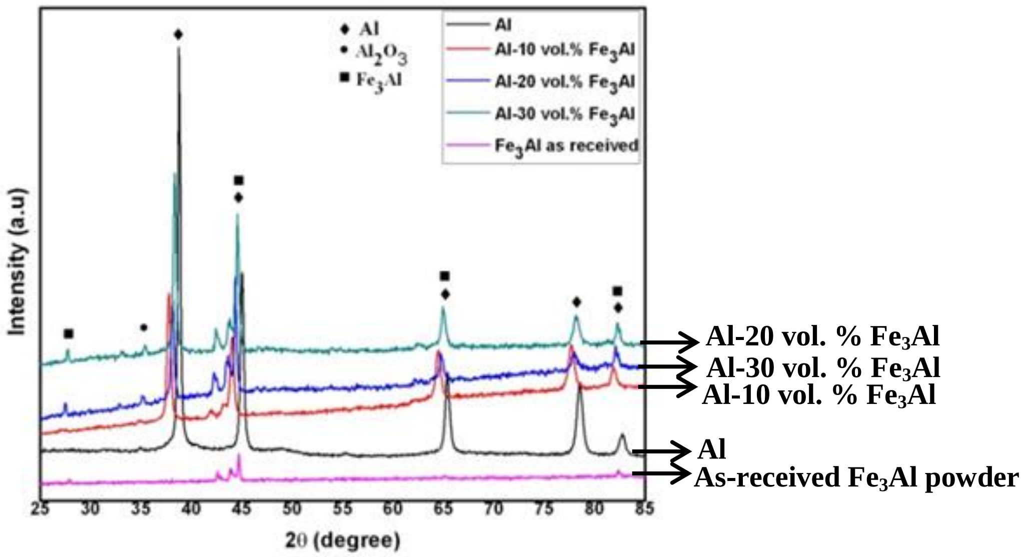

Figure 4.10: X-ray diffraction plot of as-received Fe_3Al powder, sintered pure Al, and Al-10, 20, 30 vol.% Fe_3Al sintered composites

The x-ray diffraction plot in Figure 4.10 shows the presence of Al_2O_3 in the sintered composites. Al_2O_3 peaks are seen due to the oxidation of Al by unavoidable oxygen present during sintering of the composites. No new reaction product between Fe_3Al and Al could be found in the composites. The (200) superlattice peak of Fe_3Al could be seen in the x-ray diffraction plots of Al- 20, 30 vol. % Fe_3Al sintered composites.

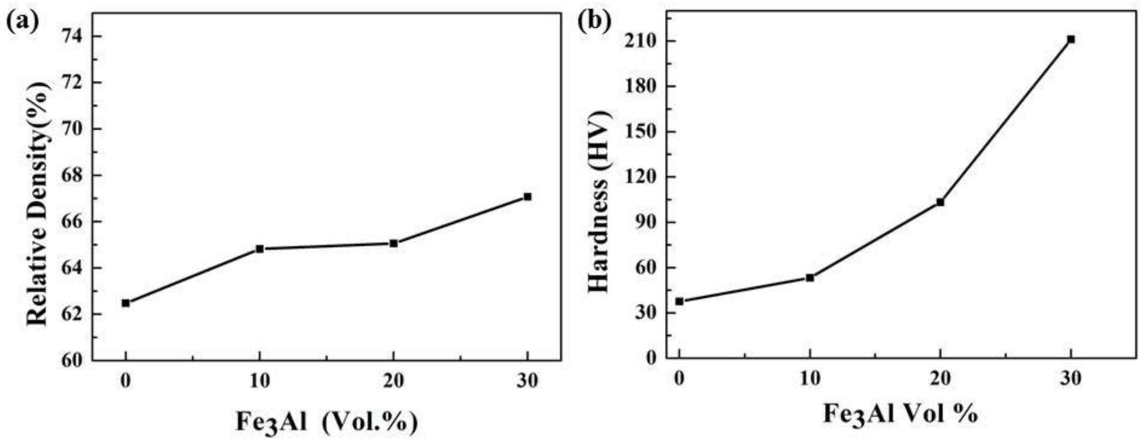

Figure 4.11: Variation of (a) relative density (b) hardness of sintered pure Al and various Al-Fe_3Al sintered composites

Table 4.2: Variation of relative density and hardness of sintered pure Al and Al-Fe_3Al composites

Fe_3Al Vol. %	Relative Density (%)	Hardness (HV)
0	62.48	37.6
10	64.82	53.27
20	65.06	103.34
30	67.07	211.13

The relative density of sintered pure Al and Al-10, 20, 30 vol. % Fe_3Al sintered composites measured by the Archimedes' method is shown in Figure 4.11 (a). It is evident from Figure 4.11 (a) that the relative density of the sintered composites increase with the increase in Fe_3Al content. The highest relative density of about 67 % was achieved in the case of Al-30 vol. % Fe_3Al sintered composite. The addition of higher vol. % of Fe_3Al in the Al-Fe_3Al composite led to higher densification of the composite. It should be noted that Al has a melting point of 660 ^{o}C and Fe_3Al has a melting point of 1540 ^{o}C. At the sintering temperature of 500 ^{o}C solid state sintering has taken place. Figure 4.11(b) shows the variation of microhardness of pure Al and Al-10, 20, 30 vol. % Fe_3Al sintered composites. It can be concluded that the hardness of the sintered Al-Fe_3Al composites increased with the increase in the content of hard Fe_3Al particulates. It should be noted that the sintered composite attains highest hardness value when the relative density of the composite also reaches a maximum value, that is, in the case of Al-30 vol. % Fe_3Al sintered composite. Therefore, the hardness of the composites typically depends on the hard Fe_3Al particle content and the sintering condition [59, 60].

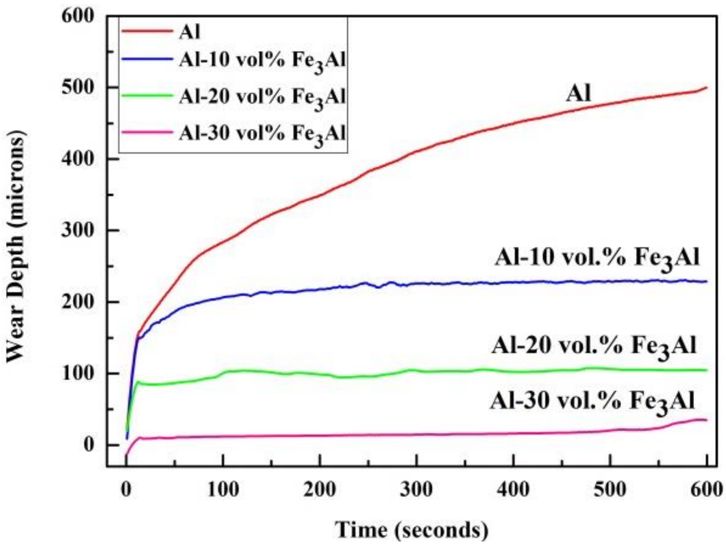

Figure 4.12: Variation of wear depth of sintered pure Al and Al-10, 20, 30 vol.% Fe_3Al sintered composites

Table 4.3: Variation of wear depth of sintered pure Al and Al-Fe_3Al composites

Fe_3Al Vol. %	Wear Depth (microns)
0	524
10	213
20	103
30	40

Wear characteristics of the sintered pure Al and the various Al-Fe_3Al sintered composites have been studied using a ball-on-plate tribometer having a diamond indenter. Wear studies have done under dry sliding conditions. In Figure 4.12 it can be seen that the wear depth of sintered composites decreases significantly with the increase in Fe_3Al content in the Al-Fe_3Al sintered composites. The sintered composites show enhanced wear resistance. The presence of the Fe_3Al particles in the Al-Fe_3Al composites provides superior wear resistance to the Al matrix.

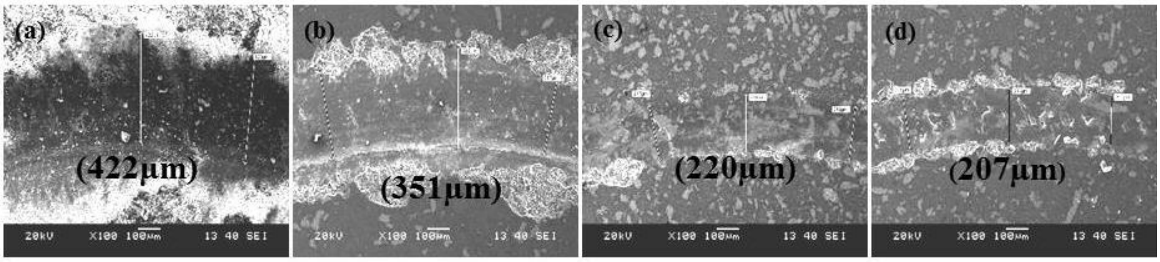

Figure 4.13: SEM images of the wear track of (a) sintered pure Al (b) Al-10 vol.% Fe_3Al (c) Al-20 vol.% Fe_3Al and (d) Al-30vol.% Fe_3Al sintered composites

This enhancement in wear resistance can be attributed to the high hardness of Fe_3Al particles as compared to soft and ductile unreinforced sintered Al. The SEM images in Figures 4.13 (a-d) show the wear track of sintered pure Al and Al-10, 20, 30 vol. % Fe_3Al sintered composites. It can be seen that the width of the wear track reduces significantly with the increase in Fe_3Al content in the Al-Fe_3Al composites [48, 61-63].

4.4 Synthesis of Fe_3Al Intermetallic Compound by Mechanical Alloying (MA)

Novel materials are being developed continuously having unique properties. An intermetallic compound consists of two or more metals in a proper stoichiometric ratio. The demand for materials having high stiffness and strength at high operating temperatures has led to greater interest in intermetallics, especially silicides and ordered intermetallics such as aluminides. Aluminides and silicides are very popular among all intermetallics because of their high oxidation and corrosion resistance due to the formation of adherent surface oxide films. According to Fleischer et al. [63-65] there are around 300 binary intermetallic compounds having melting point higher than 1500 ^{o}C. This is why intermetallics are one of the most promising structural materials at higher operating temperatures.

In the present research work iron aluminide (Fe_3Al) intemetallic compound was developed by mechanical alloying of powder mixtures of elemental Fe and Al in a proper stoichiometric ratio for upto 40 h. It is found that, during MA, Al dissolves gradually into the BCC lattice of α-Fe, resulting in the formation of Fe(Al) solid solution. Here, in our research work, the 40 h milled Fe-Al powder was isothermally heat treated at 1100 ^{o}C for a period of 2 h in order to synthesize Fe_3Al having a $D0_3$ crystal structure. During isothermal annealing of the 40 h milled $Fe_{75}Al_{25}$ powder, the order transformation from Fe(Al) to $D0_3$-Fe_3Al occurs.

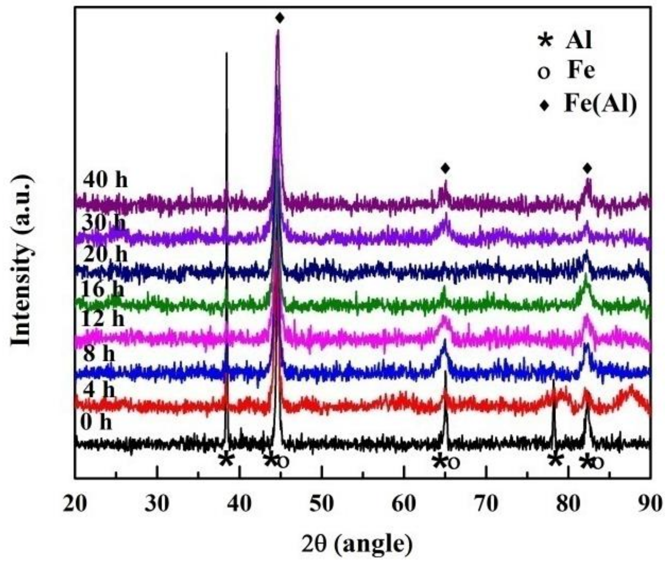

Figure 4.14: XRD patterns of $Fe_{75}Al_{25}$ powder milled for various periods of time

Figure 4.14 shows the XRD patterns of $Fe_{75}Al_{25}$ powder milled for different periods of time. In Figure 4.14 the XRD pattern of the unmilled elemental blend of Fe and Al in the stoichiometric ratio of 3:1 shows the presence of Al (111), Al (200), Al (220), Al (311), Al (222), Fe (110), Fe (200) and Fe (211) peaks. The Al (200), Al (220) and Al (222) peaks superimpose with the Fe (110), Fe (200) and Fe (211) peaks respectively. However, strong independent peaks of Al (111) and Al (311) could be seen clearly in the XRD plot. MA of the $Fe_{75}Al_{25}$ powder beyond 8 h shows the disappearance of the Al (311) peak and a sharp reduction in the intensity of the Al (111) peak. The variation in the lattice parameter of Fe was also calculated from the XRD plots of the milled $Fe_{75}Al_{25}$ powder using the Nelson-Riley function. Figure 4.15 shows the variation of the lattice parameter of Fe with milling time in the $Fe_{75}Al_{25}$ powder. After about 8 h of milling the lattice parameter of Fe was found to around 2.91 Å which is more than that of the pure Fe i.e. 2.866 Å. This is possibly due to the diffusion of Al in Fe lattice. As the radius of Al atom (1.28 Å) is less than that of Fe atom (1.40 Å), the lattice parameter of Fe(Al) should be less than that of Fe. However, the experimental results do not confirm this and the reason is not clear. This sudden rise in the lattice parameter of Fe during milling of Fe-28Al powder was also reported by Tang et al. [66]. On further milling upto 12 h the leading diffraction peaks of Fe, Fe (110), Fe (200) and Fe (211), shifted towards lower diffraction angle, which indicates the diffusion of more Al atoms in the Fe lattice.

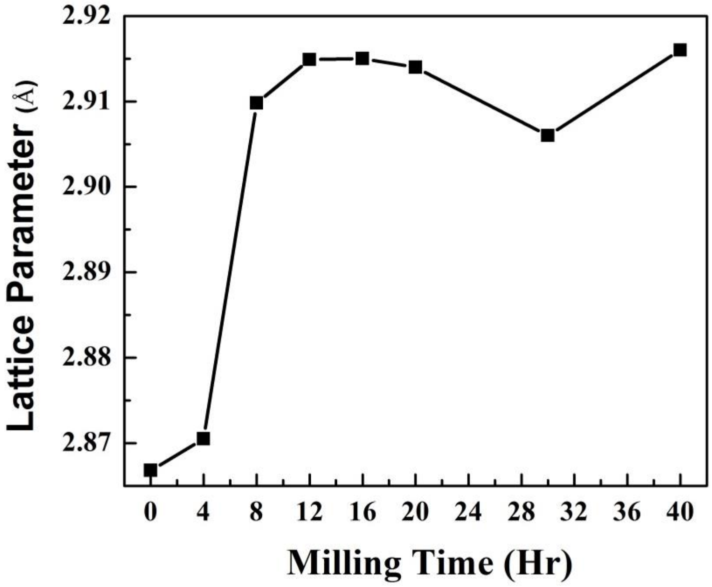

Figure 4.15: Variation of the lattice parameter of Fe after various periods of milling of $Fe_{75}Al_{25}$ powder

The crystallite size of Fe in the as-milled $Fe_{75}Al_{25}$ powder was determined using the Voigt's method. The Voigt's method is a single peak analysis method. The most intense x-ray diffraction peak has been used for crystallite size and r.m.s. strain determination [67, 68].

The broadening of the XRD peaks with the increase in milling time can be attributed to the reduction in crystallite size and increase in lattice strain. From Figure 4.16 (a) it is evident that the crystallite size of Fe could be reduced to less that is 20 nm within 8 h of milling time. However, slight rise in crystallite size could be observed between 8 to 12 h of milling. The rise in crystallite size during milling can be attributed to cold welding. The variation in crystallite size beyond 8 h of milling time shows a proper balance between cold welding and fracturing of the powder particles. The crystallite size of Fe after 40 h of milling of $Fe_{75}Al_{25}$ powder was found to be around 30 nm. Severe deformation of particles takes place during high energy milling which leads to the decrease in crystallites size and increase in the lattice strain. Figure 4.16 (b) shows the variation of lattice strain in Fe with the increase in milling time of $Fe_{75}Al_{25}$ powder. It is evident from this plot that with the increase in milling time the lattice strain in Fe also increases. From the plot in Figure 4.16 (b) a slight decrease in lattice strain is also evident during milling. During high energy milling the dislocation density is very high within the heavily strained regions. The lattice strain could decrease when the crystal disintegrates into sub grains that are separated by low-angle grain boundaries. Dislocations annihilate and recombine to form small angle grain boundaries separating the individual grains. This could result in the decrease of the lattice strain. During further milling, deformation occurs in shear bands located in previously unstrained parts of the material. The grain size decreases steadily and the shear bands coalesce. The small angle boundaries are replaced by higher angle grain boundaries, implying grain rotation and random orientation of the grains. As a result, dislocation-free nanocrystalline grains are formed. The minimum grain size attainable by milling can be attributed to the balance between the defect and dislocation structure introduced by the plastic deformation during milling and its recovery by thermal processes [35-38].

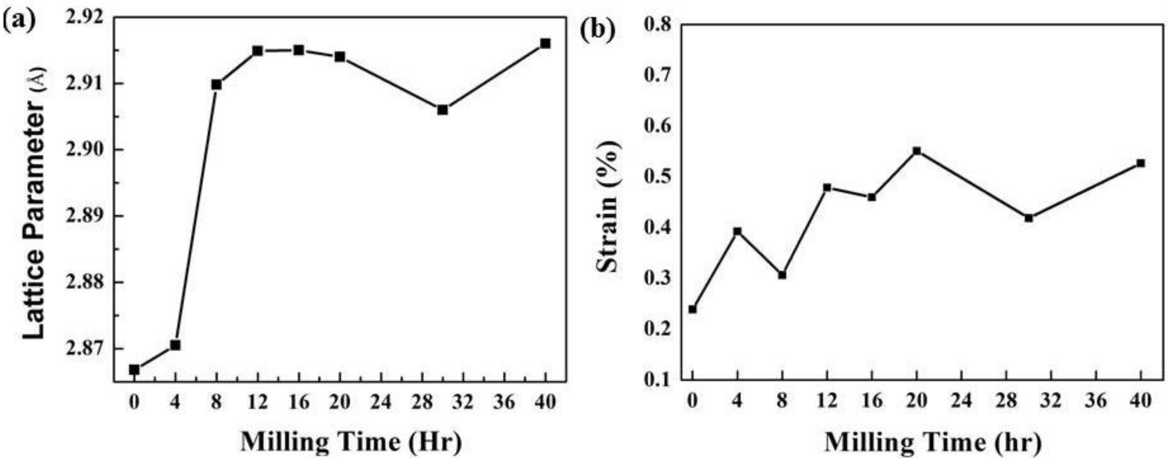

Figure 4.16: Variation of (a) crystallite size (b) strain of Fe after various periods of milling of $Fe_{75}Al_{25}$ powder

Figure 4.17 shows the XRD patterns of as-received Fe_3Al powder, 40 h milled $Fe_{75}Al_{25}$ powder and 40 h milled $Fe_{75}Al_{25}$ powder heat treated at 1100^{o}C for 2 h in Ar atmosphere. The (111) superlattice diffraction peak of $D0_3$-Fe_3Al could be detected in the XRD pattern of the 40 h milled $Fe_{75}Al_{25}$ powder heat treated at 1100 ^{o}C for 2 h. During annealing, the order transformation of the disordered Fe(Al) solid solution formed after 40 h of milling of $Fe_{75}Al_{25}$ to the ordered $D0_3$-Fe_3Al took place. The presence of the (111) superlattice peak of $D0_3$-Fe_3Al in the XRD pattern is a direct evidence of the ordered arrangement in the alloy.

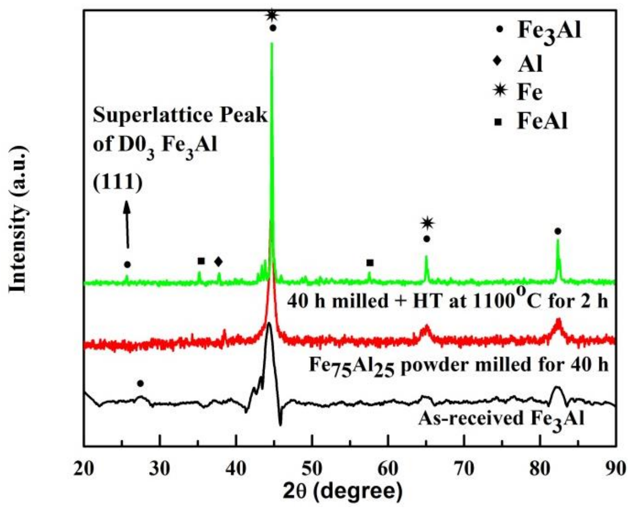

Figure 4.17: XRD patterns of as-received Fe_3Al powder, 40 h milled $Fe_{75}Al_{25}$ powder and 40 h milled $Fe_{75}Al_{25}$ powder heat treated at 1100 ^oC for 2 h

Along with the peaks of Fe_3Al, some diffraction peaks of FeAl could also be seen having very low peak intensity in the XRD pattern of the 40 h milled $Fe_{75}Al_{25}$ powder heat treated at 1100 ^oC for 2 h. The XRD pattern of as-received Fe_3Al powder in Figure 4.17 shows the (220), (400) and (422) diffraction peaks of Fe_3Al at 44^o, 64^o and 82^o respectively along with the (111) superlattice peak at 27^o.

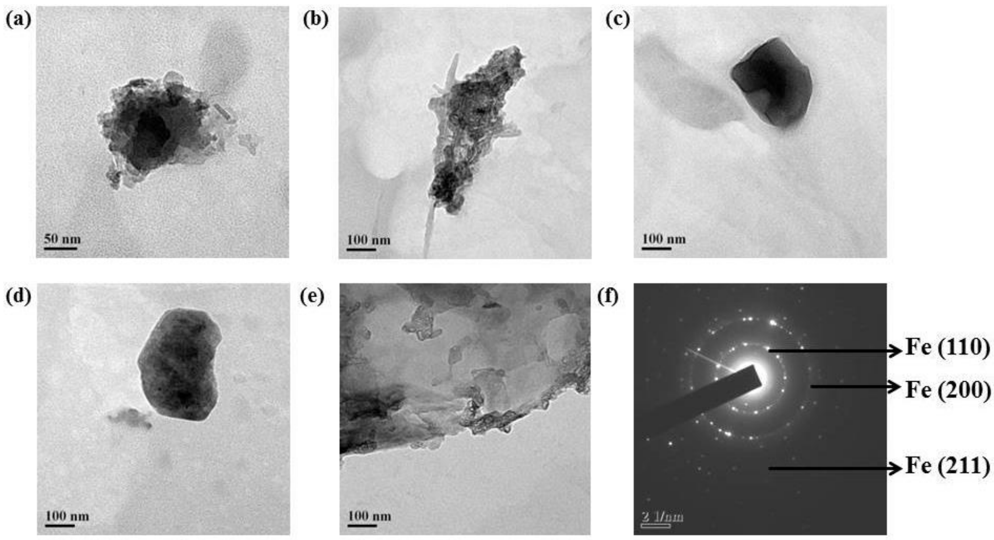

Figure 4.18: (a-e) HRTEM images (f) SAD pattern of 40 h milled $Fe_{75}Al_{25}$ powder

Figures 4.18 (a-e) are the HRTEM images of the 40 h milled $Fe_{75}Al_{25}$ powder. From the HRTEM images, it is evident that ultrafine particles having size less than 100 nm could be achieved after 40 h of milling of the $Fe_{75}Al_{25}$ powder. The SAD pattern in Figure 4.18 (f) shows sharp rings which could be indexed to the (110), (200) and (211) diffraction planes of Fe and corresponds to that of Fe(Al).

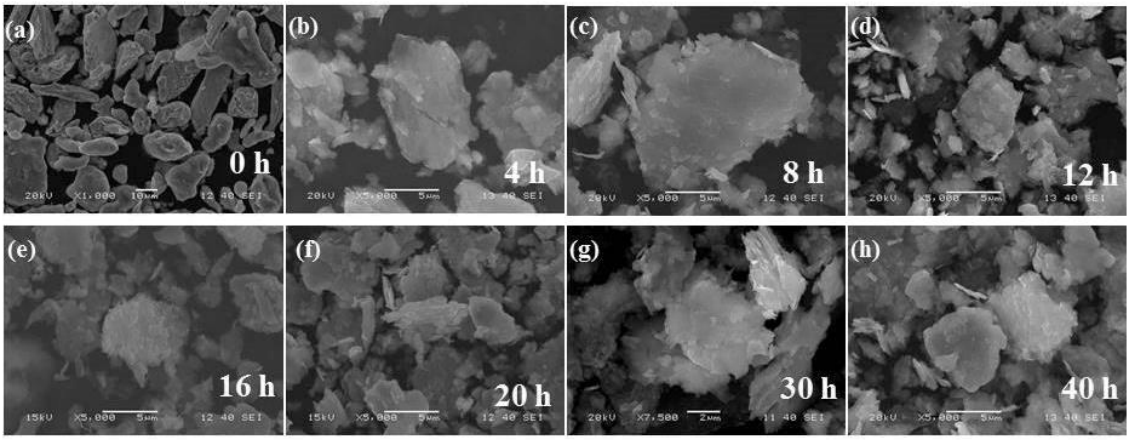

Figure 4.19: SEM images of mechanically alloyed $Fe_{75}Al_{25}$ powder after (a) 0 h (b) 4 h (c) 8 h (d) 12 h (e) 16 h (f) 20 h (g) 30 h and (h) 40 h of milling

The SEM images in Figures 4.19 (a-h) show the structural evolution of the $Fe_{75}Al_{25}$ powder after different periods of milling. During the initial period of milling, flake-like particles could be seen as is evident from the SEM images in Figures 4.19 (b, c). During MA, the powder was subjected to high-energy collision, which causes plastic deformation, cold welding and fracture. During this period, the ductile particles undergo plastic deformation. With the increase in milling time, the extent of further plastic deformation decreases. This is evident from the SEM images in Figures 4.19 (d-f). As welding is the dominant mechanism during MA, the morphology of the particles change to agglomeration of flattened particles. In the case of soft and ductile metal powders, the flattened layers overlap and form cold welds. This leads to the formation of layered composite powder particles which may consists various combinations of the starting ingredients. To reduce this cold welding between the powder particles toluene was used as a process controlling agent. At the same time, the work-hardened metal powder particles may continue to fracture. In the final stages of milling, these competing events of cold welding and fracturing continue repeatedly. As a result, a refined and homogenized microstructure could be obtained after around 30 h of milling as is evident from the SEM images in Figure 4.19 (g, h) [69-71].

Figure 4.20 shows the SEM image and the elemental maps of Al and Fe in the $Fe_{75}Al_{25}$ powder milled for various periods of time. The elemental maps of Al and Fe after different periods of milling of the $Fe_{75}Al_{25}$ powder have been analyzed in order to determine the mechanism of the formation of Fe(Al) solid solution. The alloying during the milling of $Fe_{75}Al_{25}$ powder is governed by the diffusion of the Al atoms into the Fe lattice because of the higher diffusion coefficient of the Al atoms in the Fe lattice compared with that of the Fe atoms in the Al lattice [72, 74]. Furthermore, the solid solubility of Al in Fe is enhanced due to the increase of defects in the Fe lattice and the decrease in the Fe grain size during milling. During the initial stages of milling (upto 4 h), the deformation of the Fe and Al particles mainly takes place. Both the components Fe and Al are inhomogeneously distributed and the alloying between Fe and Al is weak during this period. This is also evident from Figure 4.15 which shows only a slight increase of the lattice parameter of Fe within the initial 4 h of milling. This is possibly due to the lower amount of the Fe and Al grain boundaries and the low defect concentration in the $Fe_{75}Al_{25}$ powder during the initial period of milling which has also been reported by Tang et al. [66]. From the elemental maps of Al and Fe in Figure 4.20 it can be found that during the initial stages of milling the Al particles are deformed and surround the Fe particles constructing composite particles. Thereafter the composite particles aggregate and weld. After about 12 h of mechanical alloying complete diffusion of Al into Fe and homogenization of the composite particles takes place resulting in the formation of Fe(Al) solid solution. With further milling it could be clearly noticed from the elemental maps that both the components, Fe and Al, are well-distributed resulting in the formation of homogeneous Fe(Al) solid solution. The EDX analysis given along with the SEM images in Figure 4.20 shows the composition of the particles during milling. Initially after 4 h of milling it could be found that the concentration of Al in the particle was about 7.73 at. % (Figure 4.20 (b)). However, with progress in milling the concentration of Al in the particles was found to gradually increase and after 40 h of milling it was found to be around 28 at. % (Figure 4.20 (h)).

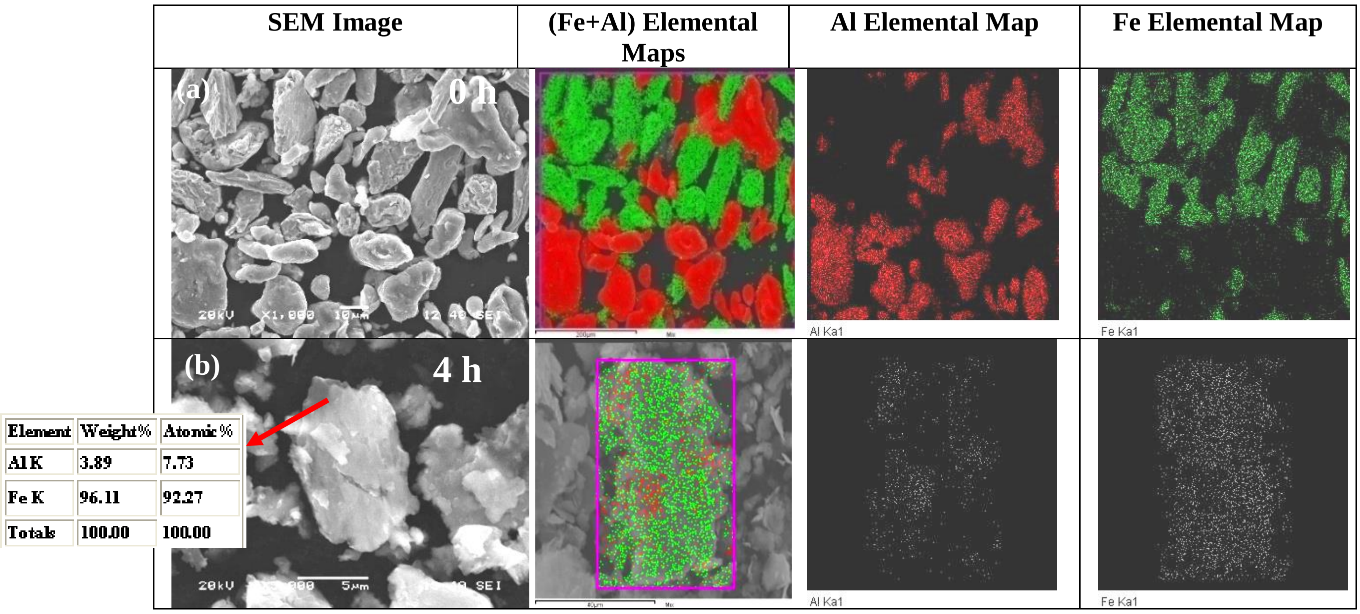

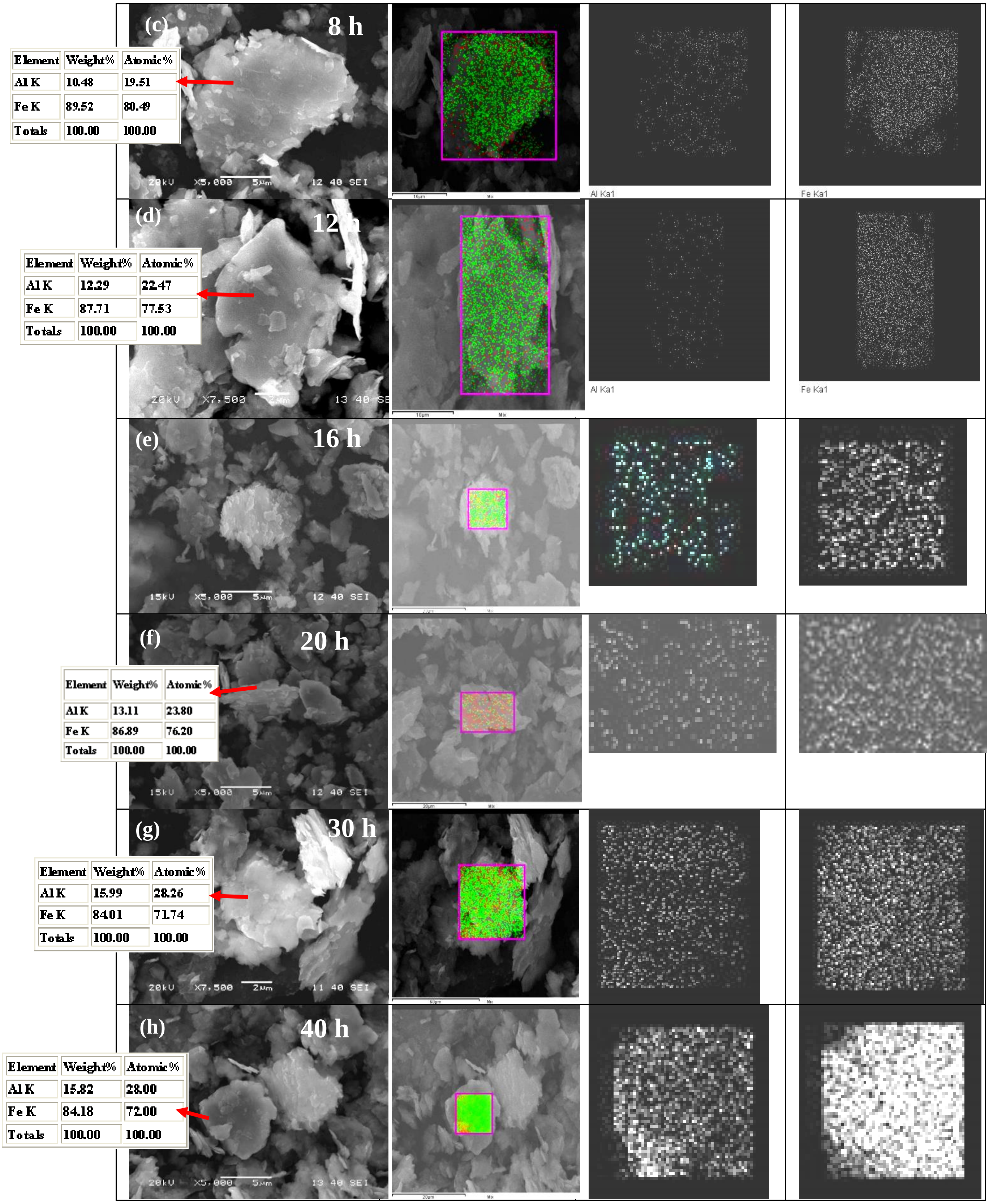

Figure 4.20: SEM image and elemental maps of (Al+Fe) combined, Al and Fe of $Fe_{75}Al_{25}$ powder milled for (a) 0 h (b) 4 h (c) 8 h (d) 12 h (e) 16 h (f) 20 h (g) 30 h and (h) 40 h

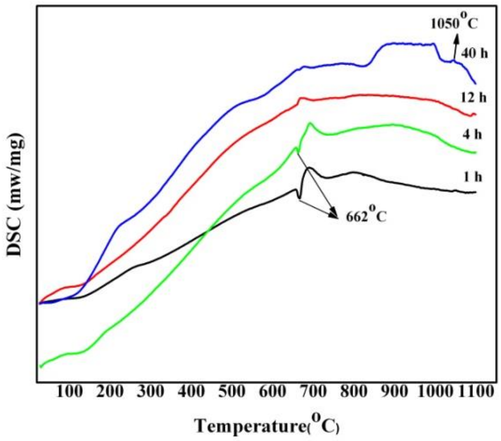

Figure 4.21: DSC analysis of 1, 4, 12 and 40 h milled $Fe_{75}Al_{25}$ powder

Figure 4.21 shows the DSC analysis of the 40 h milled $Fe_{75}Al_{25}$ powder. The DSC plot of 1 h and 4 h milled $Fe_{75}Al_{25}$ powder shows an endothermic peak at around 662 °C. This is due to the melting of the residual Al in the milled powder. Al has a melting point of 660 °C. As all the Al has not diffused in the Fe lattice to form Fe(Al) solid solution during the initial period of milling, some amount remains in the milled powder as residual Al. It should be noted that the endothermic peak at around 662 °C is not visible in the DSC plots of the 12 h and 40 h milled powder. This suggest that a significant amount of Al has dissolved into the Fe lattice after 40 h of milling and forming a complete Fe(Al) solid solution. The exothermic peak at around 1050 °C in the DSC plot of the 40 h milled powder is due the formation of the ordered $D0_3$-Fe_3Al.

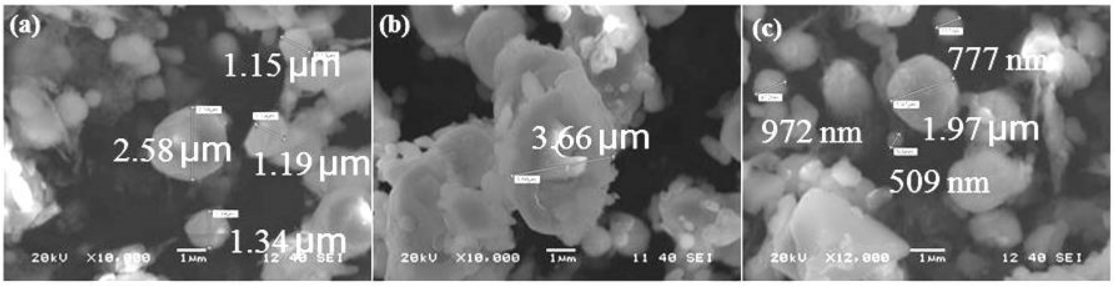

Figure 4.22: SEM images of $Fe_{75}Al_{25}$ powder milled for 40 h and heat treated at 1100°C for 2 h

From the DSC analysis in Figure 4.21 it is evident that ordered $D0_3$-Fe_3Al could be formed from the 40 h milled $Fe_{75}Al_{25}$ powder when heated to a temperature above 1100 °C. This is why in order to synthesize ordered $D0_3$-Fe_3Al the 40 h milled $Fe_{75}Al_{25}$ powder was isothermally heat treated at 1100 °C for a period of 2 h in Ar atmosphere. Figures 4.22 (a-c) are the SEM images of the Fe_3Al particles formed after the isothermal heat treatment of the 40 h milled $Fe_{75}Al_{25}$ powder. By comparing the SEM images in Figure 4.19 (h) and Figure 4.22 it is evident that the flake-like milled powder particles formed after 40 h of milling of $Fe_{75}Al_{25}$ powder changes to spherical shaped particles after subsequent heat treatment. The spherical particles have a diameter in the range of around 0.5-4 µm.

4.5 Development of Al-Fe_3Al Composites by Powder Metallurgy Route using Fe_3Al Synthesized by MA

In the present research work, the Fe_3Al intermetallic compound developed by MA of $Fe_{75}Al_{25}$ powder for a period of 40 h followed by isothermal annealing at 1100 ^oC for 2 h was also used as reinforcement for the development of Al-Fe_3Al sintered composites. The Al-10, 20, 30 vol. % Fe_3Al green compacts were developed by uniaxial cold compaction under a load of 222 MPa followed by the conventional sintering at 500 ^oC in Ar atmosphere. The various composites were characterized in order to study the effect of addition of Fe_3Al in Al matrix. The objective was also to compare the properties of the Al-Fe_3Al composites developed by using as-received commercially available Fe_3Al and Fe_3Al synthesized by MA followed by isothermal annealing.

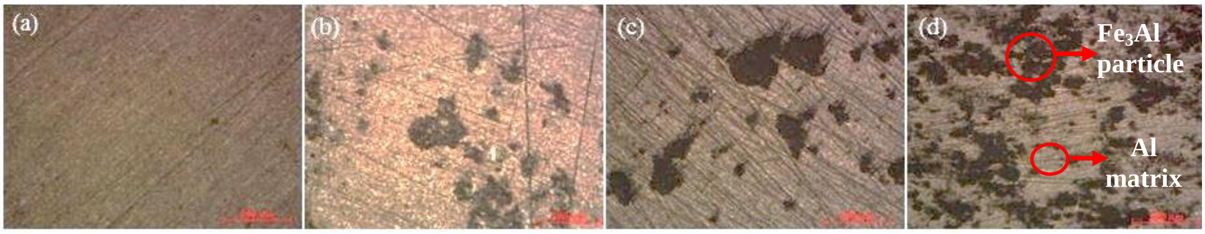

Figure 4.23: Optical images of (a) sintered pure Al and (b-d) Al-10, 20, 30 vol. % Fe_3Al sintered composites developed by using Fe_3Al synthesized by MA

Figures 4.23 (a-d) show the optical micrographs of pure Al and Al-10, 20, 30 vol. % Fe_3Al sintered composites. Here, Fe_3Al synthesized by MA has been used as reinforcement. The optical micrographs of the various composites in Figures 4.22 (b-d) show dark coloured Fe_3Al particles dispersed homogeneously in the Al matrix. The Fe_3Al particles were found irregular in shape. The sintered Al-Fe_3Al composites exhibit better homogenous and compact microstructure with the increase of Fe_3Al content in the Al matrix.

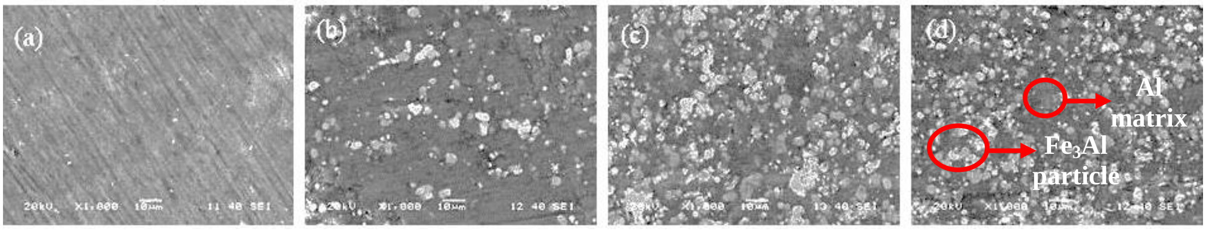

Figure 4.24: SEM images of (a) sintered pure Al and (b-d) Al-10, 20, 30 vol. % Fe_3Al sintered composites developed by using Fe_3Al synthesized by MA

Figures 4.24 (a-d) show the SEM images of pure Al and Al-10, 20, 30 vol. % Fe_3Al sintered composites. Figures 4.24 (b-d) show the unform distribution of Fe_3Al particles in the Al matrix.

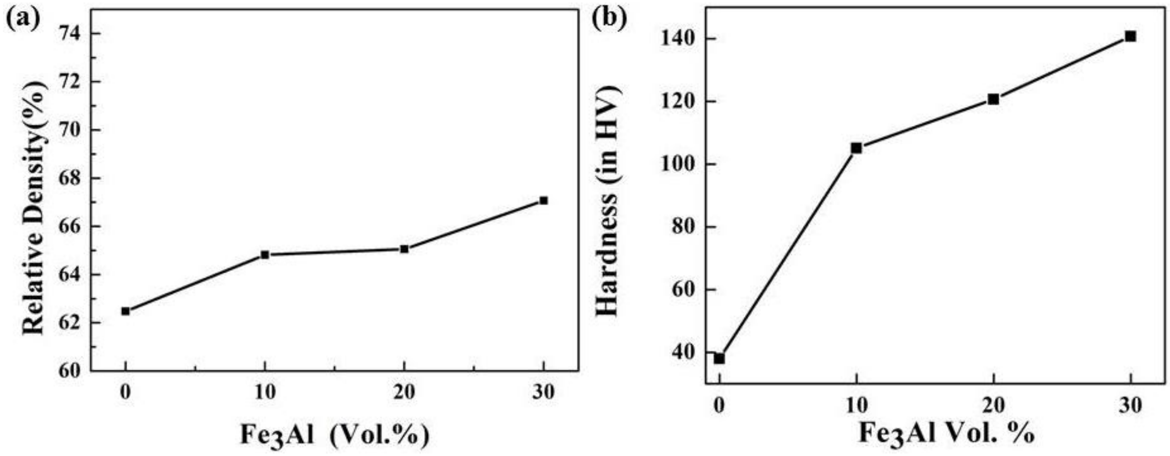

Figure 4.25: Variation of (a) relative density (b) hardness of sintered pure Al and various Al-Fe_3Al sintered composites developed by using Fe_3Al synthesized by MA

Figures 4.25 (a, b) show the varaition of relative density and microhardness of pure Al and various Al-10, 20, 30 vol. % Fe_3Al sintered composites. The relative density of pure sintered Al and various Al-Fe_3Al sintered composites were measured by the Archimedes' method shown in Figure 4.25 (a). It is evident from Figure 4.25 (a) that the relative density of the sintered composites increased with the increase in Fe_3Al content. The highest relative density of about 70 % was achieved in the case of Al-30 vol. % Fe_3Al sintered composite. Addition of higher vol. % of Fe_3Al in the Al-Fe_3Al composite led to higher densification of the composite. It should be noted that Al has a melting point of 660 ^oC and Fe_3Al has a melting point of 1540 ^oC. At 500 ^oC solid state sintering has taken place. Hardness of the composites also increased with the increase in hard Fe_3Al particle content in the sintered composites. Fe_3Al is harder than Al. While the hardness of Al is about 17 HV the hardness of Fe_3Al is nearly 338 HV. Figure 4.25 (b) shows the variation of microhardness of pure Al and Al-10, 20, 30 vol. % Fe_3Al sintered composites. From the microhardness results, it can be concluded that hardness of the sintered composites improved with the increase in Fe_3Al content. It should be noted that the sintered composite attains highest hardness value when the relative density of the composite also reaches maximum value, that is, in the case of Al-30 vol. % Fe_3Al sintered composite. Therefore the hardness value typically depends on the hard Fe_3Al particle content in the sintered composites and the sintering condition.

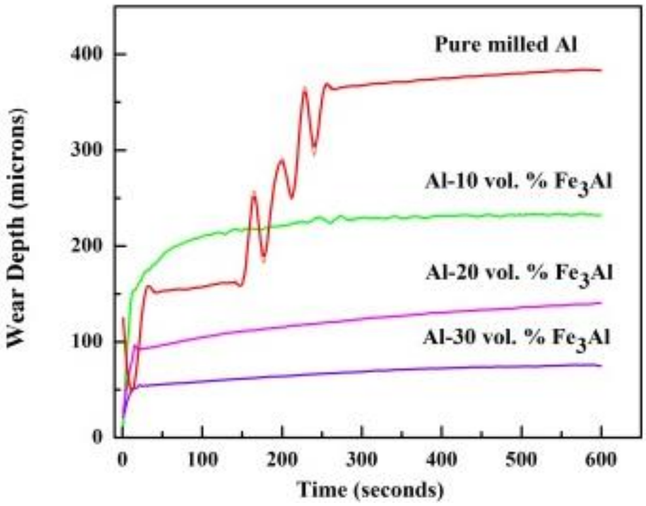

Figure 4.26: Variation of wear depth of sintered pure Al and Al-10, 20, 30 vol. % Fe_3Al sintered composites developed by using Fe_3Al synthesized by MA

Figure 4.26 shows variation of wear resistance of Pure Al and Al-10, 20, 30 vol. % Fe_3Al sintered composites where Fe_3Al powder was synthesized by milling for upto 40 h and subsequently isothermally heat treated at 1100 ^oC for 2 h in Ar atmoshphere.Wear characteristics of the consolidated specimen has been studied by ball-on-plate tribometer using a diamond indenter. Wear studies done on the various Al-Fe_3Al composites developed by powder metallurgy route under dry sliding conditions exhibit enhanced wear resistance of the sintered composites. From the results, it can be concluded that Fe_3Al particles provide superior wear resistance to Al matrix. In Figure 4.26 it can be seen that the wear depth of sintered composites significantly decerase with the increase in Fe_3Al content in the Al-Fe_3Al sintered composites.

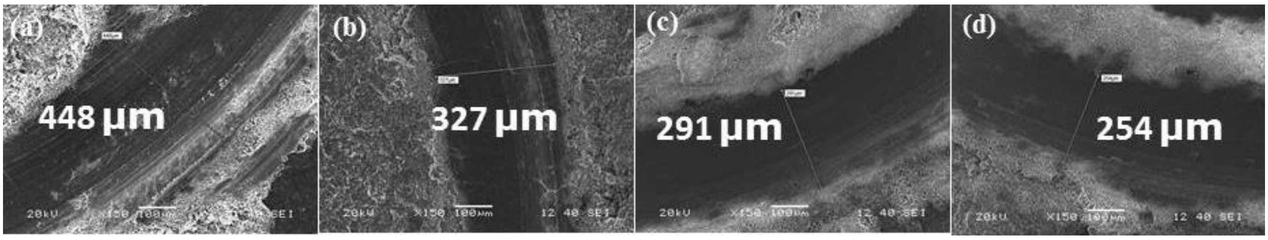

Figure 4.27: SEM images of the wear track of (a) sintered pure Al and (b-d) Al-10, 20, 30 vol.% Fe_3Al sintered composites developed by using Fe_3Al synthesized by MA

Figure 4.27 shows the SEM images of the wear track of pure Al and Al-10, 20, 30 vol. % Fe_3Al sintered composites. It is evident from the SEM images in Figures 4.27 (b-d) that the width of the wear track of Al-Fe_3Al sintered composites continuously decreases with the increase in vol. % of Fe_3Al. The highest width of the wear track of 448 µm was found in the case of pure Al sintered sample. Whereas the lowest width of the wear track of 254 µm was found in the case of Al-30 vol. % Fe_3Al sintered composite. This enhancement in wear resistance of Al-Fe_3Al sintered composites can be attributed to the high hardness of Fe_3Al particles as compared to the soft and ductile Al matrix.

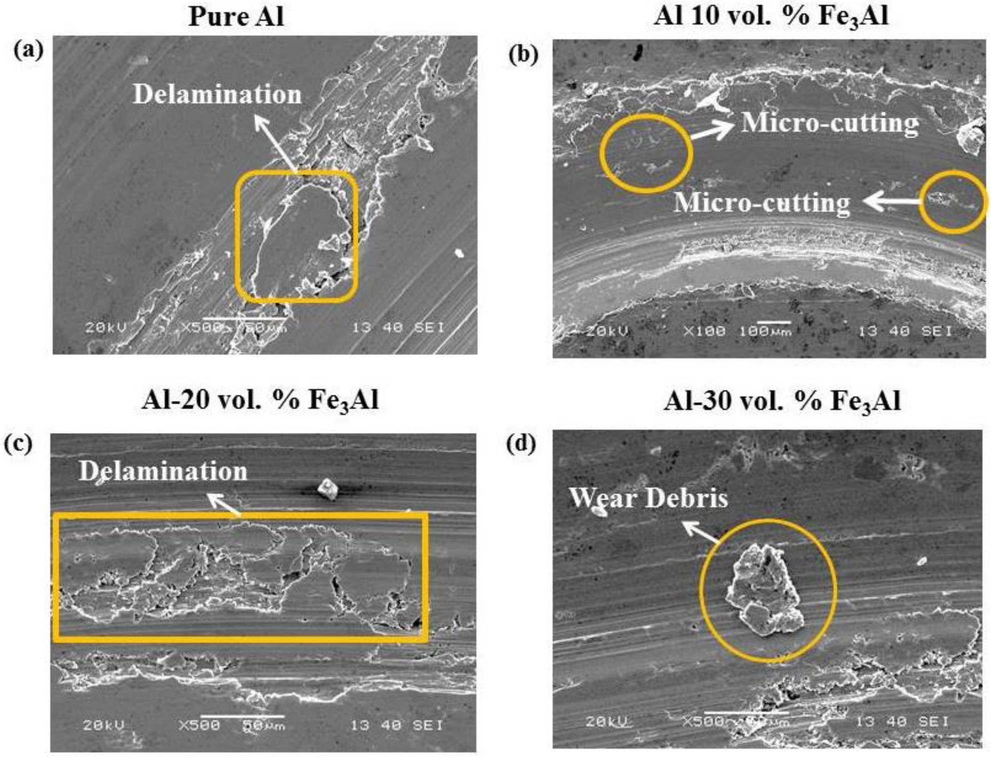

Figure 4.28: SEM images showing the wear mechanism in (a) sintered pure Al and (b-d) Al-10, 20, 30 vol.% Fe_3Al sintered composites developed by using Fe_3Al synthesized by MA

The SEM micrographs of the wear tracks of the sintered pure Al and various Al-Fe_3Al sintered composites are shown in Figures 4.28 (a-d). Al is ductile in nature and could be removed easily from the matrix in the form of wear debris. The wear debris was formed by the delamination cracks developed near the subsurface region due to the localization of plastic strain. Carcks and voids nucleate in these plastic deformation zones. Subsurface crack nucleation is followed by crack propagation which results in loose wear sheet. High contact pressure applied on the matrix during the wear test resulted in hard asperities on the counterpart penetrating and cutting deeply into the surface of the matrix, causing severe plastic deformation, which resulted in a large amount of material removal. Similar type of material removal during dry sliding wear test has also been reported by Venkateswaran et al. [47] for Cu-based MMCs reinforced with Fe_3Al intermetallic particles. Micro-cutting and ploughing were also evident in the SEM images of the wear tracks of the various Al-Fe_3Al sintered composites in Figures 4.28 (b-d). Micro-cutting was observed on the wear track due to local abrasion.

Chapter 5

Conclusions

The results of the development and characterization of Al-based metal matrix composites using as-received Fe_3Al intermetallic compound as reinforcement has been reported in this work. This work also reports the synthesis of Fe_3Al intermetallic compound by MA and the subsequent development of Al-Fe_3Al composites using the Fe_3Al synthesized by MA as reinforcement. The conclusions that have been drawn from the present research work are as follows:

1. Nanostructured Al could be synthesized by mechanical milling of elemental Al powder for a period of 20 h. The nanocrystalline nature of the 20 h milled Al was confirmed by both x-ray diffraction analysis and high resolution transmission electron microscopy. There was a gradual increase in the lattice strain with milling time due to the severe deformation of the milled powder. XRD analysis of the 20 h milled Al powder shows no trace of contamination from the milling media.
2. No new phase was formed between Al and the Fe_3Al in the sintered composites. This was confirmed from the diffraction analysis of the various composites. However, few peaks corresponding to Al_2O_3 could be seen in the x-ray diffraction plots due to the oxidation of Al.
3. The Relative density of Al-10, 20, 30 vol.% Fe_3Al sintered composites developed by powder metallurgy route using the as-received Fe_3Al as reinforcement showed slight increase with increase in Fe_3Al content. Hardness of the various Al-10, 20, 30 vol.% Fe_3Al sintered composites was also found to increase with the increase in Fe_3Al content. Al-30 vol.% Fe_3Al sintered composite showing the highest relative density of 67 % was also found to have the highest hardness value. Its hardness was found to be 211 HV.
4. Al-Fe_3Al sintered composites show significant improvement in wear resistance with the increase in the content of Fe_3Al. All the Al-10, 20, 30 vol.% Fe_3Al sintered composites show better wear resistance compared to the unreinforced pure Al sintered sample. Fe_3Al was found to be highly effective in improving the wear resistance of the Al-Fe_3Al sintered composites. This is attributed to the high hardness of Fe_3Al as compared to the soft and ductile Al matrix.
5. Fe_3Al intermetallic compound could be synthesized by mechanical alloying of $Fe_{75}Al_{25}$ powder for a period of 40 h followed by isothermal heat treatment of the

milled powder at 1100 ^oC for a period of 2 h in Ar atmosphere. The XRD analysis of the 40 h milled $Fe_{75}Al_{25}$ powder shows peaks corresponding to Fe(Al) solid solution along with the peaks Fe and Al. The XRD analysis of 40 h milled $Fe_{75}Al_{25}$ powder heat treated at 1100 ^oC for 2 h confirmed the formation of ordered $D0_3$-Fe_3Al intermetallic compound having a (111) superlattice peak at $2\theta=26^o$.

6. The elemental maps of Al and Fe in the $Fe_{75}Al_{25}$ powder milled for various periods of time suggest the gradual diffusion of Al in the Fe particles. The EDX analysis of the $Fe_{75}Al_{25}$ powder milled for various periods of time also confirms the gradual increase of Al concentration in the Fe particles. The final concentration of Al in the Fe particle after 40 h of milling of $Fe_{75}Al_{25}$ powder was found to be around 28 at.%.
7. Al-10, 20, 30 vol. % Fe_3Al composites were developed by powder metallurgy route using Fe_3Al synthesized by MA as reinforcement. The relative density of the various Al-Fe_3Al sintered composites shows an increase with the increase in Fe_3Al content in the Al-Fe_3Al composites. The hardness of the various composites also show an increase with the increase in Fe_3Al content. The Al-30 vol.% Fe_3Al sintered composite showing the highest relative density of 70 % was also found to have the highest hardenss value. Its hardness value was found to be 140 HV.
8. Al-Fe_3Al sintered composites developed by powder metallurgy route using Fe_3Al synthesized by MA as reinforcement show significant improvement in wear resistance with the increase in Fe_3Al content. All the Al-10, 20, 30 vol. % Fe_3Al sintered composites show better wear resistance compared to the unreinforced pure Al sintered sample.
9. By comparing the properties of the Al-Fe_3Al composites developed using as-received Fe_3Al and Fe_3Al synthesized by MA, it was found that Al-30 vol. % Fe_3Al sintered composite developed using the as-received Fe_3Al shows higher hardness as well as superior wear properties as compared to the Al-30 vol. % Fe_3Al sintered composite developed using Fe_3Al synthesized by MA.

Scope for Further Research

1. Iron aluminide (Fe_3Al) is one of the major aluminides of interest to the scientific community. Fe_3Al can be used as reinforcement in various other soft and ductile metal matrix composites, like copper based composites, to increase its wear resistance and hardness. These composites could be used in various applications in automotive and aerospace industries.

2. The effect of addition of other aluminides, like FeAl, Ni_3Al and NiAl in the development of MMCs could also be studied.
3. High temperature properties of the developed composite can also be studied.

Bibliography

[1] D. Hull and T. W. Clyne. *An Introduction to Composite Materials*. Cambridge University Press, 1996.

[2] B. Harris. *Engineering Composite Materials*. IOM, 1999.

[3] L. E. Asp and E. S. Greenhalgh. Structural Power Composites. *Composites Science And Technology*, 101:41-61, 2014.

[4] K. K. Chawla. *Composite Materials: Science and Engineering.* Springer Science & Business Media, 1998.

[5] L. J. Broutman. *Composite Materials*. Academic Press, 1974.

[6] R. Everett. *Metal Matrix Composites: Processing and Interfaces*. Academic Press, 2012.

[7] M. Demirel and M. Muratoglu. The Friction and Behaviour of Cu-Ni_3Al Composites by Dry Sliding. *Materials and Technology*, 45(5):401-406, 2011.

[8] X. H. Wang, M. Zhang and B. S. Du. Fabrication in-situ TiB_2-TiC-Al_2O_3 Multiple Ceramic Particles Reinforced Fe-Based Composite Coatings by Gas Tungsten Arc Welding. *Tribology Letters*, 41(1):171-176, 2011.

[9] M. Abbasi, M. Azabdeh and S.A. Sajjadi. Evolution of Manufacturing Parameters in Al-Ni_3Al Composite Powder Formation using Blending and Mechanical Milling Process. *Journal of Material Science*, 45: 4524-4531, 2010.

[10] Z. Sadeghian, M. H. Enayati and E. P. Beiss, In-situ Production of Al–TiB_2 Nanocomposite by Double-Step Mechanical Alloying. *Journal of Material Science*, 44:2566-2572, 2009.

[11] T. Varol and A. Canakci. The Effect of Type and Ratio of Reinforcement on the Synthesis and Characterization Cu-based Nanocomposites by Flake Powder Metallurgy. *Journal of Alloys and Compounds*, 649:1066-1074, 2015.

[12] S. N. Alam. Synthesis and Characterization of W–Cu Nanocomposites Developed by Mechanical Alloying. *Materials Science and Engineering: A*, 433:161-168, 2006.

[13] J. S. Benjamin. Dispersion Strengthened Superalloys by Mechanical Alloying. *Metallurgical and Materials Transactions A*, 1(10):2943–2951, 1970.

[14] C. Suryanarayana. Mechanical Alloying and Milling. *Progress in Materials Science*, 46(1-2):1-184, 2001.

[15] C. C. Koch. Materials Synthesis by Mechanical Alloying. *Annual Review of Materials Science*, 19(1):121-143, 1989.

[16] J. S. Benjamin and T. E. Volin. The Mechanism of Mechanical Alloying. *Metallurgical Transactions*, 5(8):1929–1934, 1974.

[17] K.Chawla and M. Meyers. *Mechanical Behavior of Materials.2nd*, Cambridge University Press, 2008.

[18] F. L. Matthews and R. D. Rawlings. *Composite Materials: Engineering and Science*. Elsevier, 1999.

[19] S. M. Choi and H. Awaji. Nanocomposites-A New Material Design Concept. S*cience and Technology of Advanced Materials*, 6(1):2-10, 2005.

[20] K. U. Kainer. *Basics of Metal Matrix Composites.* Wiley-VCH Verlag GmbH & Co. KGaA, 2006.

[21] D. B. Miracle. Metal Matrix Composites - From Science to Technological Significance. *Composites Science and Technology*, 65 (15-16):2526–2540, 2005.

[22] K. U. Kainer. *Metal Matrix Composites: Custom-made Materials for Automotive and Aerospace Engineering*. John Wiley & Sons, 2006.

[23] M. Balasubramanian. *Composite Materials and Processing*. Taylor and Francis Group LLC, 2014.

[24] S. Suresh, A. Mortensen and A. Needleman. *Fundamentals of Metal-matrix Composites*. Butterworth-Heinemann, 1993.

[25] M. K. Surappa and P. K. Rohatgi. Preparation and Properties of Cast Aluminium-

Ceramic Particle Composites. *Journal of Materials Science*, 16:983-993, 1981.

[26] R. M. German, P. Suri, and S. J. Park. Review: Liquid Phase Sintering. *Journal of Materials Science*, 44(1):1-39, 2009.

[27] R. M. German. *Powder Metallurgy Science.* Metal Powder Industries Federation, 1994.

[28] P. Ramakrishanan. *Powder Metallurgy*. New Age International, 2007.

[29] K. K. Gan, N. Chen, Y. Wang, and M. Y. Gu. SiC/Cu Composites with Tungsten Coating Prepared by Powder Metallurgy. *Materials Science and Technology*, 23(1):119-122, 2007.

[30] J. R. Pickens. Review Aluminium Powder Metallurgy Technology for High Strength Applications. *Journal of Materials Science*, 16:1437-1457, 1981.

[31] G. E. Totten, L. Xie and K. Funatani. *Handbook of Mechanical Alloy Design.* CRC Press, 2003.

[32] P. C. Angelo and R. Subramanian. *Powder Metallurgy: Science, Technology and Applications.* PHI Learning Pvt. Ltd., 2008.

[33] N. S. Stoloff. *Physical Metallurgy and Processing of Intermetallic Compounds*. Chapman & Hall, 1996.

[34] R. Mitra. *Structural Intermetallics and Intermetallic Matrix Composites*. CRC Press, 2015.

[35] B. S. Murty and S. Ranganathan. Novel Materials Synthesis by Mechanical Alloying/Milling. *International Materials Reviews*, 43(3):101-141, 1998.

[36] D. Oleszak and P. H. Shingu. Mechanical Alloying in the FeAl System. *Materials Science and Engineering: A*, 181-182:1217–1221, 1994.

[37] M. H. Enayati and M. Salehi. Formation Mechanism of Fe_3Al and FeAl Intermetallic Compounds during Mechanical Alloying. *Journal of Materials Science*, 40:3933-3938, 2005.

[38] Z. G. Liu, J. T. Guo, L. L. He and Z. Q. Hu. Formation of B2 Intermetallic NiAl and FeAl by Mechanical Alloying. *Nanostructured Materials*, 4(7):787-794, 1994.

[39] S. S. Nayak, M. Wollgarten, J. Banhart, S. K. Pabi and B. S. Murty. Nanocomposites and an Extremely Hard Nanocrystalline Intermetallic of Al-Fe Alloys Prepared by Mechanical Alloying. *Materials Science and Engineering: A*, 527:2370-2378, 2010.

[40] B. Huang, K. N. Ishihara and P. H. Shingu. Metastable Phases of Al-Fe System by Mechanical Alloying. *Materials Science and Engineering: A*, 231:72-79, 1997.

[41] Y. Zou, S. Saji and K. Kusabiraki. Fast Amorphization and Crystallization in Al-Fe binary System by High-Energy Ball Milling. *Materials Research Bulletin*, 37:123-131, 2002.

[42] Z. Adabavazeh, F. Karimzadeh and M. H. Enayati. Synthesis and Structural Characterization of Nanocrystalline (Ni, Fe)$_3$Al Intermetallic Compound Prepared by Mechanical Alloying. *Advanced Powder Technology*, 23:284–289, 2012.

[43] M. Krasnowski, A. Grabias and T. Kulik. Phase Transformations During Mechanical Alloying of Fe-50% Al and Subsequent Heating of the Milling Product. *Journal of Alloys and Compounds*, 424:119-127, 2006.

[44] E. Bonetti, G. Scipione, G. Valdrf, S. Enzo, R. Frattini, P. P. Macri. A Study of Nanocrystalline Iron And Aluminium Metals and Fe_3Al Intermetallic by Mechanical Alloying. *Journal of Materials Science,* 30:2220-2226, 1995.

[45] E. Bonetti, G. Valdre, S. Enzo, G. Cocco and I. Soletta. Nanostructured Fe_3Al Intermetallic Obtained by Mechanical Alloying and Thermal Ageing. *Nanostructured Materials*, 2(4):369-375, 1993.

[46] J.P. Tu, L. Meng and M.S. Liu. Friction and Wear Behavior of Cu-Fe_3Al Powder Metallurgical Composites in Dry Sliding. *Wear,* 220(1):72-79, 1998.

[47] K. Venkateswaran, M. Kamaraj and K. Prasad Rao. Dry Sliding Wear of a Powder Metallurgy Copper-based Metal Matrix Composite Reinforced with Iron Aluminide Intermetallic Particles. *Journal of Composite Materials,* 4(14):1713-1728, 2007.

[48] F. Velasco, C. E. da Costa and J. M. Torralba. Mechanical Properties and Wear Behaviour of PM Aluminium Composite Reinforced with Fe_3Al Particles. *Powder Metallurgy,* 45(3):247-250, 2002.

[49] T. Raghu, R. Sundaresan, P. Ramakrishnan and T. R. Rama Mohan. Synthesis of Nanocrystalline Copper-Tungsten Alloys by Mechanical Alloying. *Materials Science and Engineering: A*, 304-306:438-441, 2001.

[50] Q. Balci, D. Agogullari, H. Gokce, I. Duman and M. L, Ovecoglu. Influence of TiB_2 Particle Size on the Microstructure and Properties of Al matrix Composites Prepared via Mechanical Alloying and Pressureless Sintering. *Journal of Alloys and Compounds*, 586:S78-S84, 2014.

[51] D. K. Koli, G. Agnihotri and R. Purohit. A Review on Properties, Behaviour and Processing methods for Al- Nano Al_2O_3 Composites. *Procedia Materials Science*, 6:567-589, 2014.

[52] N. Qj, M. Hu, Z. Wang, Z. Lu and C. Xie. Synthesis of Al-Fe_3Al Core-Shell Intermetallic Nanoparticles by Chemical Liquid Deposition Method. *Advanced powder Technology*, 4:926-931, 2013.

[53] N. Lakshmi, V. Sebastian and K. Venugopalan. Clustering in Heusler Alloys. *Springer Proceedings in Physics,* 122:21-35, 2009.

[54] Tomoyuki and Kakeshita. *Progress in Advanced Structural and Functional Materials Design.* Springer Science & Business Media, 2013.

[55] S. S. Rehman, W. Ji, S. A. Khan, M. Asif, Z. Fu, W. Wang, H. Wang, J. Zhang and Y. Wang. Microstructure and Mechanical Properties of B_4C Based Ceramics with Fe_3Al as Sintering Aid by Spark Plasma Sintering. *Journal of European Ceramic Society*, 34:2169-2175, 2014.

[56] Y. Zhumagaliev, S. Baisanov, A. Chekimbaev and N. Nurgali. *Other Ferroalloys Fundamentals*. The Twelfth International Ferroalloys Congress Sustainable Future, Helsinki, Finland, 2010.

[57] J. Wang, J. Xing, Z. Qiu, X. Zhi and L. Cao. Effect of Fabrication Methods on Microstructure and Mechanical Properties of Fe_3Al based Alloys. *Journal of Alloys and Compounds,* 488(1):117-122, 2009.

[58] J. Li, Q. Liu, R. X. Shi, Y. Wen and Ya. S. Yin. Preparation and Mechanical Properties of $Fe_3Al(Ti)$/Tic Composites. *Journal of Materials Processing Technology,* 208:105-110, 2008.

[59] T. Jiang. Investigation of Microstructure and Property of Fe_3Al/Al_2O_3

Composites. *Advanced Materials Research*, 150-151:1409-1412, 2011.

[60] L. X. Pang, K.N. Sun, S. Ren, C. Sun, R. H. Fan and Z. H. Lu. Fabrication and microstructure of Fe_3Al matrix Composite Reinforced by Carbon Nanotube. *Materials Science and Engineering: A,* 447(1-2):146-149, 2007.

[61] D. Sundararaman. Investigatoon of Tribological Properties of Functionally Graded as-Cast MMC. *International Journal of Advanced Materials Manufacturing and Characterization*, 1(1): 2012.

[62] T. Itoi, S. Mineta, H. Kimura, K. Yoshimi and M. Hirohashi. Fabrication and wear Properties of Fe_3Al-Based Composites. *Intermetallics*, 18(11):2169–2177, 2010.

[63] J. Cheng, B. Yin, Z. Qiao, J. Yang and W. Liu. Mechanical and Dry-Sliding Tribological Properties of Fe_3Al Based Composites Reinforced by Novel $W_{0.5}Al_{0.5}C_{0.5}$ Particulates. *Materials& Design*, 66:67-76, 2015.

[64] R. L. Fleischer. Intermetallic Compounds for High-Temperature Structural Use Unique Iridium and Ruthenium Compounds. *Platinum Metals Review*, 36(3):138-145, 1992.

[65] J. H. Westbrook and R. L. Fleischer. *Intermetallic Compounds, Principles and Practice*. John Wiley & Sons, Inc., 2002.

[66] W. M. Tang, Z. X. Zheng, H. J. Tang, R. Ren and Y. C. Wu. Structural Evolution and Grain Growth Kinetics of the Fe-28Al Elemental Powder During Mechanical Alloying and Annealing. *Intermetallics,* 15:1020-1026, 2007.

[67] D. Balzar and H. Ledbetter. Voigt-Function Modeling in Fourier Analysis of Size-and Strain-Broadened X-ray Diffraction Peaks. *Journal of Applied Crystallography*, 26:97-103, 1993.

[68] D. Balzar, N. Audebrand, M. R. Daymond, A. Fitch, A. Hewat, J. I. Langford, A. Le Bail, D. Louer, O. Masson, C. N. McCowan, N. C. Popa, P. W. Stephens, and B. H. Toby. Size-Strain Line-Broadening Analysis of the Ceria Round-Robin Sample. *Journal Of Applied Crystallography,* 37(6):911–924, 2004.

[69] M. Ramezani and T. Neitzert. Mechanical Milling of Aluminum Powder using Planetary Ball Milling Process. *Journal of Achievements in Materials and Manufacturing Engineering*, 55(2):790-798, 2012.

[70] C. S. Torres and L. Schaeffer. Effect of High Energy Milling on the Microstructure and Properties of WC-Ni Composite. *Materials Research*, 13(3), 2010.

[71] M. Sherif El-Eskandarany. *Mechanical Alloying for Fabrication of Advanced Engineering Materials*. William Andrew Publishing, Norwich, New York, U.S.A., 2001.

[72] R. L. White. The use of Mechanical Alloying in the Manufacture of Multi Filamentary Superconductor Wire. Ph.D. Thesis, Stanford University, USA, 1979.

[73] R. B. Schwarz and C.C. Koch. Formation of Amorphous Alloys by the Mechanical Alloying of Crystalline Powders of Pure Metals and Powders of Intermetallics. *Applied Physics Letters*, 49(3):146-148, 1986.

[74] H. G. Jiang, R. J. Perez and M. L. Lau. Formation Kinetics of Nanocrystalline Fe - 4 wt. % Al Solid Solution during Ball Milling. *Journal of Materials Research*, 12:1429-1432,1997

Dissemination

Journal Articles

1. Deepankar Panda, Lailesh Kumar and Syed Nasimul Alam. Development of Al-Fe_3Al Nanocomposite by Powder Metallurgy Route. *Materials Today: Proceedings*, 2(4-5):3565-3574, 2015.

2. Synthesis of Fe_3Al Intermetallic Compound by Mechanical Alloying and a study of the Mechanical Properties of Al-Fe_3Al composites. (Under Review)

3. Influence of Fe_3Al volume fraction on the strength and investigation of dissipative mechanism in Al-Fe_3Al composites. (Manuscript Under Preparation)

Conference Presentation

1. D. Panda, L. Kumar, S. N. Alam. Development of Al-Fe_3Al Nanocomposite by Powder Metallurgy Route, Presented at ICMPC 2015, GRIET Hyderabad.

2. Pallabi Bhuyan, Syed Nasimul Alam, Deepankar Panda, Lailesh Kumar, Harspreet Singh. Synthesis and Characterization of Cu-Fe_3Al Composites Using Powder Metallurgy Route, to be Presented at ICMPC 2016, GRIET Hyderabad.

Curriculum Vitae

Name Deepankar Panda

Date of Birth 11.04.1991

Permanent Address Mohapatra Complex, Jagda
Rourkela, Odisha
India
Pin: 769042

E-mail ID deepankar.panda66@gmail.com

Languages Known English, Hindi, Odia

Educational Qualifications:

Year	Degree/Certificate	Institution	Percentage/CGPA
2013	Bachelor of Technology (Metallurgical and Materials Engineering)	IGIT Sarang	7.9/10
2008	C.H.S.E	Govt. Autonomous College Panposh, Rourkela	66%
2006	H.S.C	Vivekananda Shiksha Sadan, Sec-1, Rourkela	85.2%